"SIMULTANEOUS MULTI - POINT SENSING USING EXTERNAL PHASE MODULATION BRILLOUIN OPTICAL CORRELATION DOMAIN TECHNIQUE THROUGH LOCK-IN DETECTION "

A THESIS

Submitted by

SUSMIT DATTA (EE17M085)

for the award of the degree

in

M.TECH (MICRO ELECTRONICS AND PHOTONICS), EE5

DEPARTMENT OF ELECTRICAL ENGINEERING

INDIAN INSTITUTE OF TECHNOLOGY MADRAS, CHENNAI

MAY 2019

THESIS CERTIFICATE

This is to certify that the thesis titled ***"SIMULTANEOUS MULTI-POINT SENSING USING EXTERNAL PHASE MODULATION BRILLOUIN OPTICAL CORRELATION DOMAIN TECHNIQUE THROUGH LOCK-IN DETECTION"*** *Submitted by* ***SUSMIT DATTA (EE17M085)*** *to the* ***INDIAN INSTITUTE OF TECHNOLOGY MADRAS, CHENNAI****, for the award of the degree of* ***MASTER OF TECHNOLOGY (M.TECH)****, is a bonafide record of the research work carried out by him under my Supervision. The contents of this thesis, in full or in parts have not been submitted to any other Institute or University for the award of any degree or diploma.*

Dr. BALAJI SRINIVASAN

Project Guide

Professor

Dept. of Electrical Engineering

IIT MADRAS, 600036

Place: Chennai

Date: May 2019

ACKNOWLEGEMENTS

I would like to express my heartiest gratitude towards my guide **Dr. BALAJI SRINIVASAN** for constantly guiding me throughout my project tenure and motivating me.

I would also take the opportunity to thank research scholar Ramya selvaraj (Dept. of Engineering Design, IIT MADRAS to lend me the AMETEK 7225 lock-in amplifier) which I used extensively for my project.

Finally, I would like to thank Dr. Bhargav Somepalli, who paved the way for this project and has been a building block of the Brillouin sensing set-up here in our lab. Excerpts of the codes are taken from his thesis work which I carried forward, modified and verified accordingly with controlled experiments with the lock-in amplifier. Also, I would thank Abhinav Agarwal, M.S scholar for all our technical discussions & brainstorming sessions which helped me manoeuver my technical & experimental skills.

Last but not the least; I would like to thank my parents for giving me such a wonderful opportunity to pursue my M.TECH here in IIT MADRAS.

ABBREVIATIONS

AWG:	Arbitrary waveform generator
BFS:	Brillouin frequency shift
BGS:	Brillouin gain spectrum
BOCDA:	Brillouin optical correlation domain analysis
BOTDA:	Brillouin optical time domain analysis
BPF:	Band pass filter
DAQ:	Data acquisition
EDFA:	Erbium-doped fiber amplifier
EOM:	Electro-optic modulator
ESA:	Electrical spectrum analyser
FBG:	Fiber Bragg grating
FM:	Frequency modulation
FUT:	Fiber under test
FWHM:	Full-width at half maximum
LIA:	lock-in amplifier
PD:	Photo detector
PM:	Phase modulator
PS:	Polarization scrambler
RF:	Radio frequency
SBS:	Stimulated Brillouin scattering
SHM:	Structural health monitoring
SMF:	Single mode fiber
SNR:	Signal-to-noise ratio

NOTATION

f_B	Brillouin frequency shift
$\Delta\nu_B$	Brillouin gain bandwidth
Γ_B	Reciprocal of the phonon lifetime
ω_c	Angular frequency of optical carrier
ω_p	Angular frequency of pump lightwave
ω_s	Angular frequency of probe/Stokes lightwave
$\vec{k_p}$	Wavevector of pump lightwave
$\vec{k_s}$	Wavevector of Stokes lightwave
$\vec{q}$	Wavevector of acoustic wave
Ω_B	Angular frequency of acoustic wave
V_a	Velocity of acoustic wave in optical fiber
θ	Angle between pump and Stokes waves
g_B	Brillouin gain
g_0	Peak Brillouin gain
P_{th}	Brillouin threshold power
λ_p	Wavelength of pump lightwave
ν_p	Frequency of pump lightwave
ν_S	Frequency of Stokes lightwave
ν_{AS}	Frequency of anti-Stokes lightwave
P_{pump}	Instantaneous pump power
P_{probe}	Instantaneous probe power
f_{pump}	Instantaneous pump frequency
f_{probe}	Instantaneous probe frequency
f_c	Frequency of optical carrier
dz	Space step size used in simulations
dt	Time step size used in simulations
c	Velocity of light in vacuum
n	Effective refractive index of single-mode optical fiber
v_g	Group velocity of light in optical fiber

LIST OF FIGURES

2.04 : only 1 correlation peak formed at 750 m

2.05 : 3 correlation peaks formed at 500m, 1500 m and 2500 m

2.06 : zeroth order correlation peak formed at 1500 m

2.07 : shift in zeroth order correlation peak

2.08 : Interaction of pulsed pump and CW probe in BOCDA for spatial mapping of correlation profile.

2.09 : zeroth order correlation peak formed at 1.09 km

2.10,2.11,2.12 corresponding BGS plot

3.01 BOCDA experimental setup

3.02 Spatial mapping experimental setup

3.03 Spatial mapping of 0th order correlation peak for varying peak-to-peak voltages,

f_m= 10 kHz, pulse width=200 ns

3.04 simulation and experimental verification of zeroth order correlation peak for f_m =10 kHz, Δf =0.532 GHz corresponding to 0.7v pp

3.05 Investigating dependence of width of correlation peak on pump pulse width

3.06 Dependence of width of correlation peaks on the pump pulse width

3.07 Tunability of the 1st order correlation peak with change in fm. Pulse width=100ns

3.08 LOCK-IN amplifier working

3.09 Typical AM spectrum

3.10 Time domain plot of AM signal fed-in

3.11 Received Spectrum of AM signal through Lock-in detection

3.12 A sinusoid and a noise signal is fed in to Lock-in amplifier

3.13 spectrum of two Sinusoids of different frequencies

3.14 Lock-in detection of square pulse

3.15 Internal generated frequency vs time

3.16: externally generated frequency vs time

TABLE OF CONTENTS

CHAPTER 3 (BOCDA EXPERIMENTS & STATIC STRAIN SENSING)

CHAPTER 4 CONCLUSIONS

Appendix

Chapter1: INTRODUCTION

Structural Health Monitoring

Civil infrastructure is generally the most capital intensive of national investments of any country and has a long service life expectation. It is also costly to maintain and difficult to replace. To ensure structural integrity and safety as infrastructure ages and deteriorates, routine manual visual inspections must be performed to inspect for signs of degradation and corrosion. These techniques are time-consuming and labour intensive and expose operators to health and safety hazards associated with confined spaces work. Moreover, the economic impact of structural deficiency is reflected by costs of reconstruction. Well-maintained structures are more durable, and an increase in durability decreases the direct economic losses. Hence monitoring of capital-intensive structures such as bridges, dams, oil and gas pipelines, wind turbines and aero-space vehicles is very essential. Health monitoring of these structures consists of determining the location and severity of damage in the structures [Chang et al. (2003)]. The data resulting from a monitoring programme are used to optimize the operation, maintenance, repair and replacing of the structure.

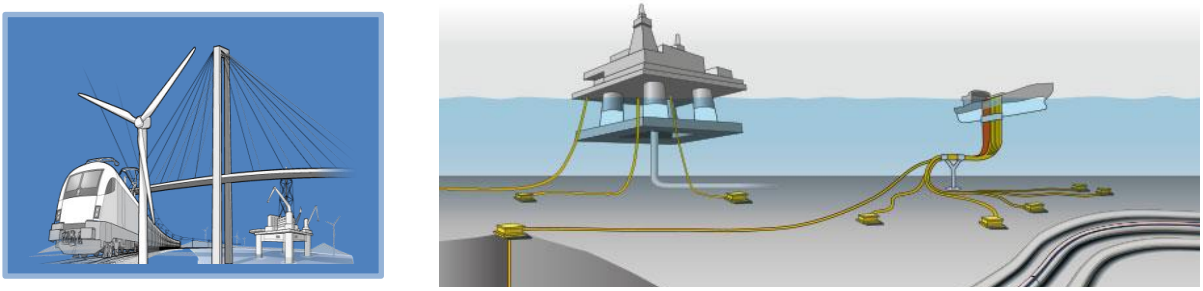

Fig.1.01: Capital Intensive Civil Structures such as bridges, oil & gas pipelines (Source: Internet)

This requirement, broadly classified as structural health monitoring (SHM), is key to maximizing the service life of the above-mentioned structures. One such example is SHM of aero-space vehicles. Specifically, because of the harsh and dynamic environment that such vehicles undergo, they require constant monitoring for early detection of abnormalities. Conventional SHM practice involves schedule-based inspection of critical parameters in the

structure at regular intervals. Such a practice needs the aircraft to be idle for that duration, which results in a loss of potential revenue. Moreover, scheduled inspections performed at regular intervals are not sufficient to detect abnormalities that are evident only in a dynamic environment. Hence, there is a need for in-situ monitoring - continuous assessment of health while the plane is in flight.

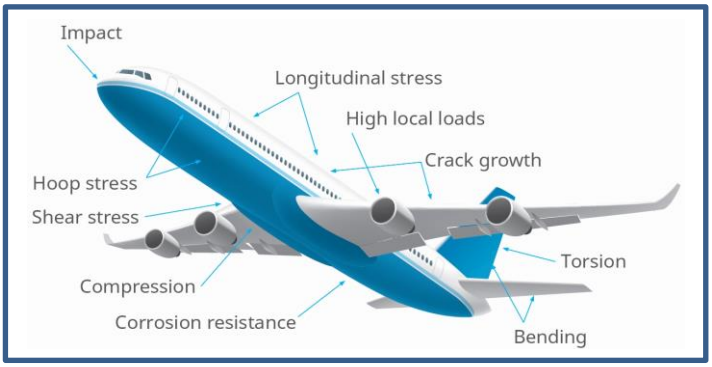

Fig.1.02: Load profile of an aircraft & need for in-situ SHM (Source: Internet)

Ultrasound detection and vibration monitoring constitute the earliest precursors for defects/failures in a structure. Of these two, vibrations are relatively easier to detect as they consist of low frequency signals. However, as in the case of any other structural parameter, the defects and the ensuing vibrations may happen at any location in a structure and hence would have to be detected using distributed sensing techniques.

Developments and advancement in the SHM technologies have gained very immense interest due to its capability to provide improvement in quality, safety and reliability by drastically minimising the human involvement. Especially, for the large structures like oil/gas pipelines and overhead power cables, manual checking for damage like cracks or leakage is time consuming. The conventional methods that use mechanical and electrical sensors would require a large number of point sensors to collect the information throughout the region of interest. The complexity can be greatly reduced by choosing a distributed sensing scheme which can deliver the information about the location and perturbation simultaneously.

What is Distributed Sensing? Need for Distributed Sensing

Distributed sensing is a technology that enables continuous, real-time measurements along the entire length of a fibre optic cable. Unlike traditional sensors that rely on discrete sensors measuring at pre-determined points, distributed sensing does not rely upon manufactured sensors but utilises the optical fibre. The optical fibre is the sensing element without any additional transducers in the optical path.

The conventional methods that use mechanical and electrical sensors would require a large number of point sensors to collect the information throughout the region of interest. The

complexity can be greatly reduced by choosing a distributed sensing scheme which can deliver the information about the location and perturbation simultaneously. Such a dedicated distributed sensing system is required for condition monitoring of both the built environment and the natural one, as they are subjected to the ravages of time, weather, temperature, stress/strain, crack and leakages. Most of the time, the process of deterioration often starts much before any signs are visible and with the knowledge based on damage mechanics and behaviour laws it is possible to determine the prognosis and the health management of the structure such as organization of maintenance, repair operations.

In addition to the disadvantages/issues mentioned above, the conventional sensors are susceptible to Electro-magnetic Interference (EMI) and many practical implementation challenges in harsh temperature conditions. This can be overcome by taking the advantages of the intrinsic properties of the fiber optic cable for the sensing purpose in which the hair thick fiber can replace 1000s of point sensors. The optical properties such as intensity, polarization, phase or frequency of the transmitted signal varies with the external perturbations and hence can be used to extract the desired information about the physical quantities such as temperature, strain, rotation, humidity, acoustic field and much more.

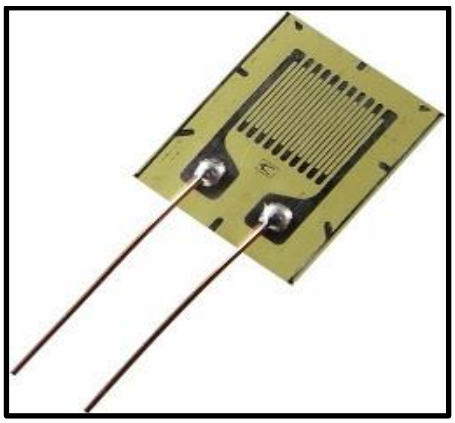

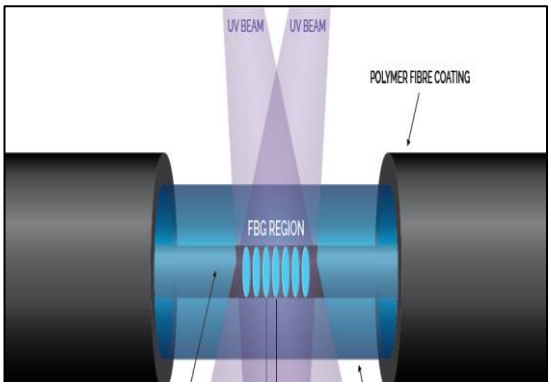

Fig.1.03: Strain Gauge (point Sensor) **Fig.1.04:** FBGs (Quasi-Distributed Sensors)

Sensor systems based on strain gauges are not only vulnerable to electro-magnetic interference (EMI) but also suffer from implementation challenges across bends and edges of the structures. In contrast, optical fiber sensors exhibit attractive features such as negligible EMI, localized probe, ability to bend over corners, and are amenable to distributed sensing.

A typical optical fiber sensor system for structural health monitoring consists of an optical fiber either bonded or embedded within the structure such that the perturbation to be monitored is experienced by the optical fiber .One of the major concerns in the real field implementation of optical fiber sensors is the reliability of the sensors which relates to efficient transfer of the measurand from the structure of interest to the optical fiber. For applications such as SHM of aircrafts made of composites, the optical fibers are being

embedded within the material which improves the robustness of the sensor. Among optical fiber sensors, those based on fiber Bragg gratings have advantages of compact size, low cost and good linearity, and are widely used for monitoring of damages and cracks [Guo et al. (2011)]. However, since FBGs are essentially point sensors they can at best be used as quasi-distributed sensors and cannot be used to monitor large structures that require sensing at multiple arbitrary locations.

Among distributed fiber sensors, those based on stimulated Brillouin scattering (SBS) have proved to be a competent technology for distributed measurements as they have the ability to provide strain/temperature information over >100 km with sub-meter spatial resolution. Traditionally, the long distance distributed sensing requirement is met by the BOTDA technique while cm/mm resolution distributed sensing is done by correlation techniques like BOCDA where the SBS interaction is localized to sensing locations.

Scattering of light in optical fiber:

When light propagates in an inhomogeneous media (like optical fiber), several spectral components can be observed corresponding to the scattered light, each representing a specific type of interaction between incident light and matter (silica). These are Rayleigh scattering, Raman scattering & Brillouin scattering.

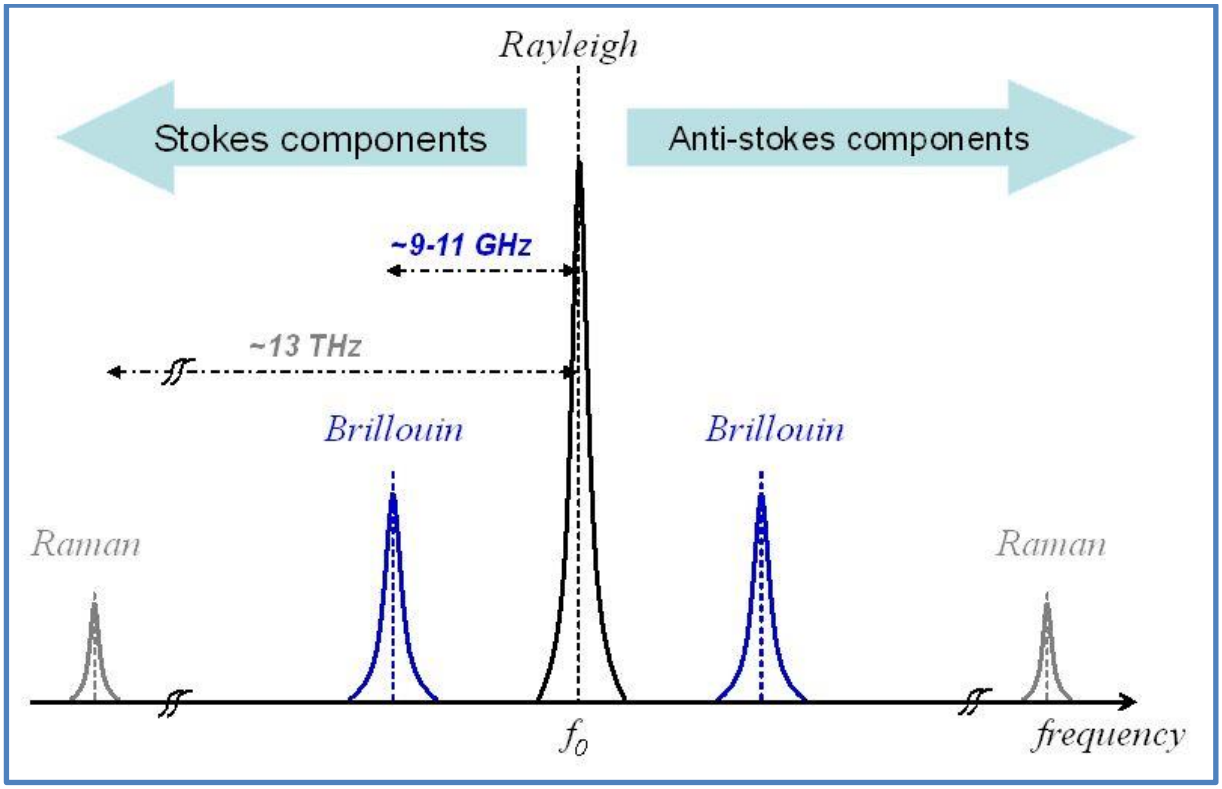

Fig.1.05: Spectrum of Scattered light in an Optical fiber

Rayleigh scattering: Elastic scattering resulting from interaction of light with non-propagating density fluctuations. It is scattering from the particles, which are much smaller than the wavelength of the light. Rayleigh-wing scattering is scattering from fluctuations in the orientation of anisotropic molecules and it is also considered as an elastic process.

Raman scattering: The origin of the Raman scattering lies in interaction of light with vibrational modes of the molecules in the media which can be better described as scattering from the fluctuations of the medium entropy. Due to the fast vibration and small momentum of these modes scattered light has a larger frequency shift of the order of THz.

Brillouin scattering: Brillouin scattering is generated due to the thermal motion of molecules. Inside the medium density fluctuation creates acoustic phonons, and interaction of incident light with these phonons results in Brillouin scattering. The relatively low frequencies of the acoustic modes results in frequency shift of the order of 10 GHz from that of the incident light. The spectral components of the scattered light having frequencies down-shifted from that of the incident are denoted as Stokes component and that those are up-shifted are denoted as anti-Stokes components. A large number of distributed sensors are proposed relying on the above scattering process with appropriated interrogation scheme and post processing methods.

Why Brillouin sensing a potential candidate for strain and temperature sensing?

Rayleigh scattering being an elastic form of scattering doesn't perturb to strain/temperature variations in an optical fiber. In Rayleigh scattering, the signal increases linearly with pressure, something that can be made use of in certain applications. Through the dependence of the signal on density, the temperature of a gas may be determined, other things that can be measured with Rayleigh scattering is density and pressure.

On the other hand, if the scattered frequency is higher than the frequency of incident light, the molecules of the medium transfer part of their energy to the photons of incident light. This generates photons with higher energy that is known as Anti-Stokes (AS) scattering. Below figure illustrates the light interaction with the optical fiber with respective mechanisms of scattering observed as a function of the light wavelength, where the peak intensity depends on the temperature (T). As shown in **Fig.1.06,** the intensity of the Raman upshifted frequency component (Anti-Stokes light) exhibits a strong dependence on the temperature, while the downshifted frequency component (Stokes light) is slightly temperature dependent.

Unlike the vibrational modes which responds to only the thermal perturbations, the material density and hence the acoustic phonons changes with the change in both temperature and strain. Thus, temperature and strain information can be estimated by analysing the Brillouin scattered light and this property makes this inelastic scattering

process a potential candidate for distributed temperature and strain sensor. The rest of the thesis focuses on the distributed fiber optic sensors using Brillouin scattering

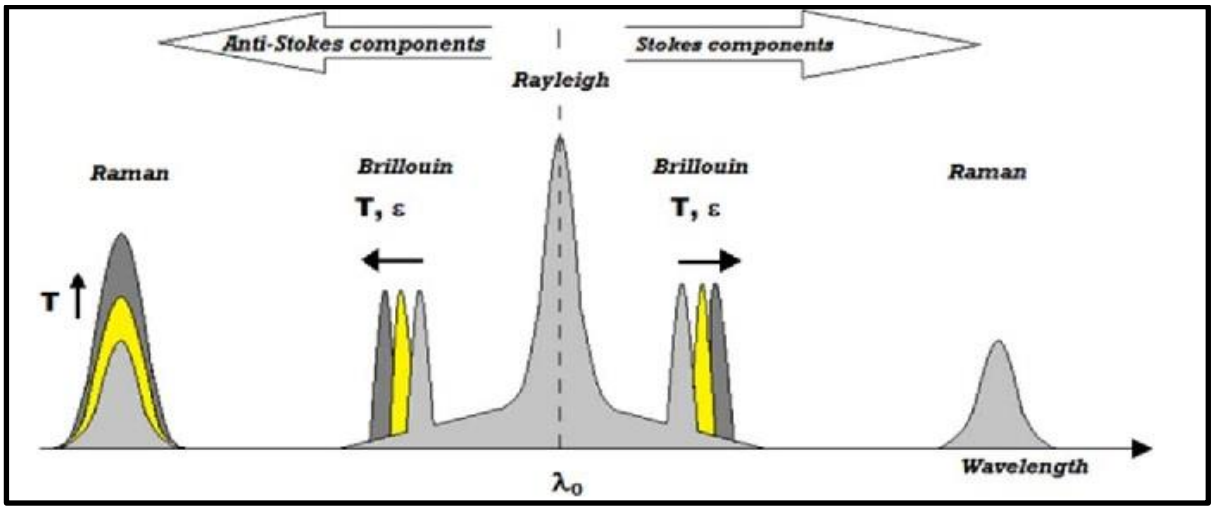

Fig.1.06: Dependence of Scattered Spectrum on physical parameters like (temperature/strain)

Depending on the power level of the exciting pump signal, the scattering can be branched into spontaneous and stimulated regime

1. Spontaneous Brillouin scattering (SpBS):

Spontaneous Brillouin scattering (SpBS) is caused by the propagation of density fluctuations which results from spontaneous pressure-waves (acoustic waves), arising from thermal agitation of the medium. In spontaneous Brillouin scattering, incident light with low intensity launched from one end of the fiber scatters from the acoustic phonons generated by the thermal motion of materials in the medium. The random motion of these acoustic phonons results in scattered light with different propagation directions and frequencies. The scattering process can be explained in quantum mechanical formulation as annihilation of a pump photon which creates a Stokes photon and simultaneous generation of acoustic phonon.

1.1 Conservation of momentum and energy

The interaction between the light waves and the acoustic wave can be treated as Bragg diffraction, in which the acoustic wave modulates the density of the medium, which causes a sine-shape modulation of the dielectric permittivity (added to its mean value). This Bragg grating, moving at the speed of sound, scatters the incident light wave with a frequency

shift due to the Doppler Effect. By imposing the Bragg conditions for the conservation of energy and momentum, we obtain the following two cases:

1. When the incident light wave and the acoustic wave propagate in the same direction we have a backscattered Stokes wave:

$$\omega_s = \omega_p - \Omega_B$$

$$k_s = k_p - q$$

2. When the incident lightwave and the acoustic wave propagate in opposite directions we have a backscattered anti-Stokes wave:

$$\omega_{as} = \omega_p + \Omega_B$$

$$k_{as} = k_p + q$$

The frequencies and wave numbers are linked by the dispersion relations for both acoustic waves and electromagnetic waves

$$|q| = \frac{\Omega}{V_A} \quad , \quad |k_p| = \frac{n\omega_p}{c} \quad , \quad |k_s| = \frac{n\omega_s}{c}$$

For a given incident lightwave, the acoustic-wave frequency and wave vector must each have a particular value for any scattering direction **Fig1.07**. Shows the relation between the wave vectors and the scattered angle.

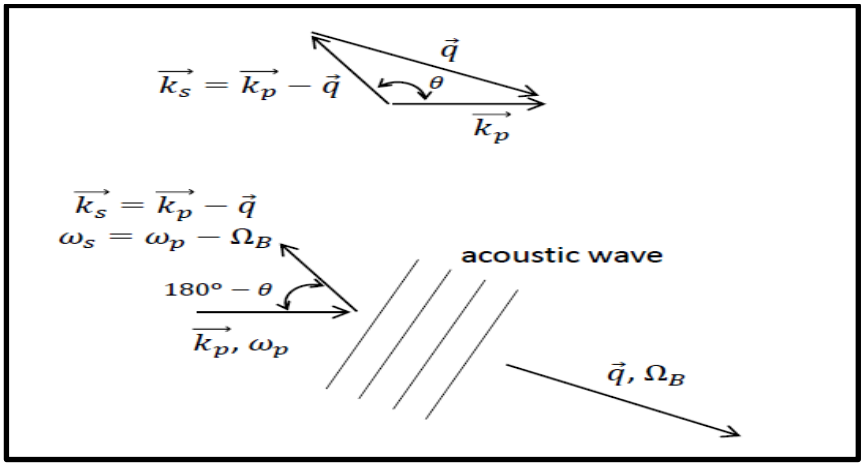

Fig.1.07: Momentum Conservation & Scattering process of Stokes Component

Since Ω_B is much smaller than ω_p, ω_s is nearly equal to ω_p and therefore $|k_s| \approx |k_p|$ and we have:

$$\Omega_B = 2\,|K_P|\,V_a \sin(\frac{\theta}{2}) = \Omega_B = 2\,V_a \frac{2\pi n}{\lambda_p} \sin(\frac{\theta}{2})$$

Where, λ_p is the wavelength of the pump light wave. Note that in a single-mode optical fiber (SMF), only two directions of propagation are possible, $\theta = 0^\circ$ corresponding to forward scattering where Ω_B =0 (scattered light has same frequency as pump wave) and then $\theta = 180^\circ$ corresponding to backward scattering where $\Omega_B \neq 0$ (scattered and pump frequencies are different). Thus, the shift in frequency referred to as Brillouin frequency shift in a single-mode optical fiber corresponding to backward scattering can be derived from Eq. above as:

$$f_B = \frac{\Omega_B}{2\pi} = \frac{2nV_a}{\lambda_p}$$

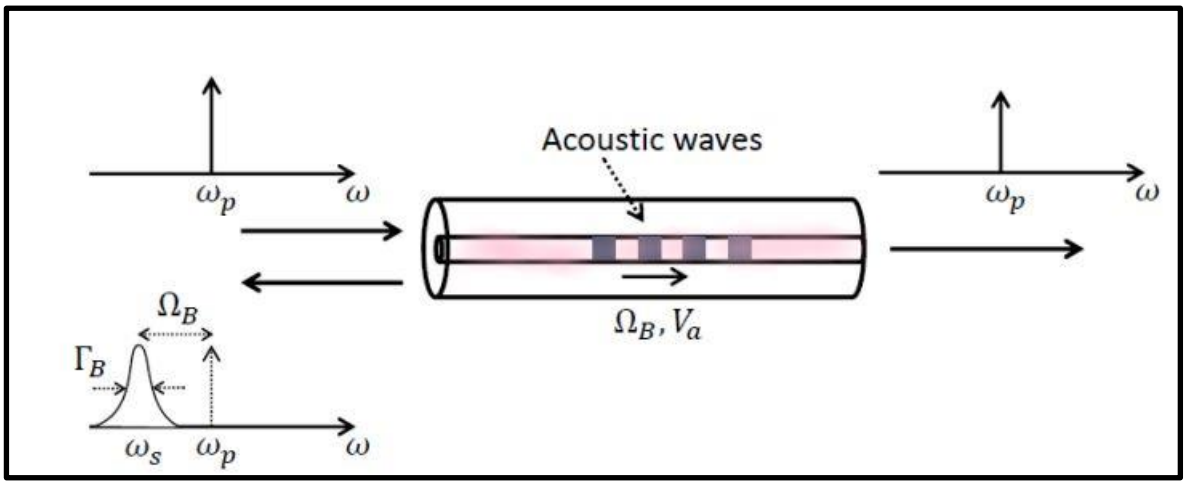

Fig.1.08: Illustration of back scattering in optical fiber

f_B is proportional to the acoustic velocity, V_a. Thus, the Stokes scattering can be visualized as scattering of pump from a retreating acoustic wave. Due to finite lifetime of the acoustic phonons, the spectrum of the backscattered signal - referred to as Brillouin gain spectrum (BGS) has a finite width - referred to as Brillouin gain bandwidth ($\Delta\nu_B$) of FWHM 30 MHz as shown in above **Fig.1.08** . Due to the exponential decay of the acoustic waves, the Brillouin gain spectrum has a Lorentzian shape given by [Agrawal (2007)]

$$g = g_o \frac{(\Gamma_B / 2)^2}{(\Gamma_B / 2)^2 + (\Omega - \Omega_B)^2}$$

Where, $\Gamma_B = 2\pi\Delta\nu_B$ is the reciprocal of phonon lifetime and g_o is the peak Brillouin gain which is of the order 2.5×10^{-11} m/W for Silica fibers.

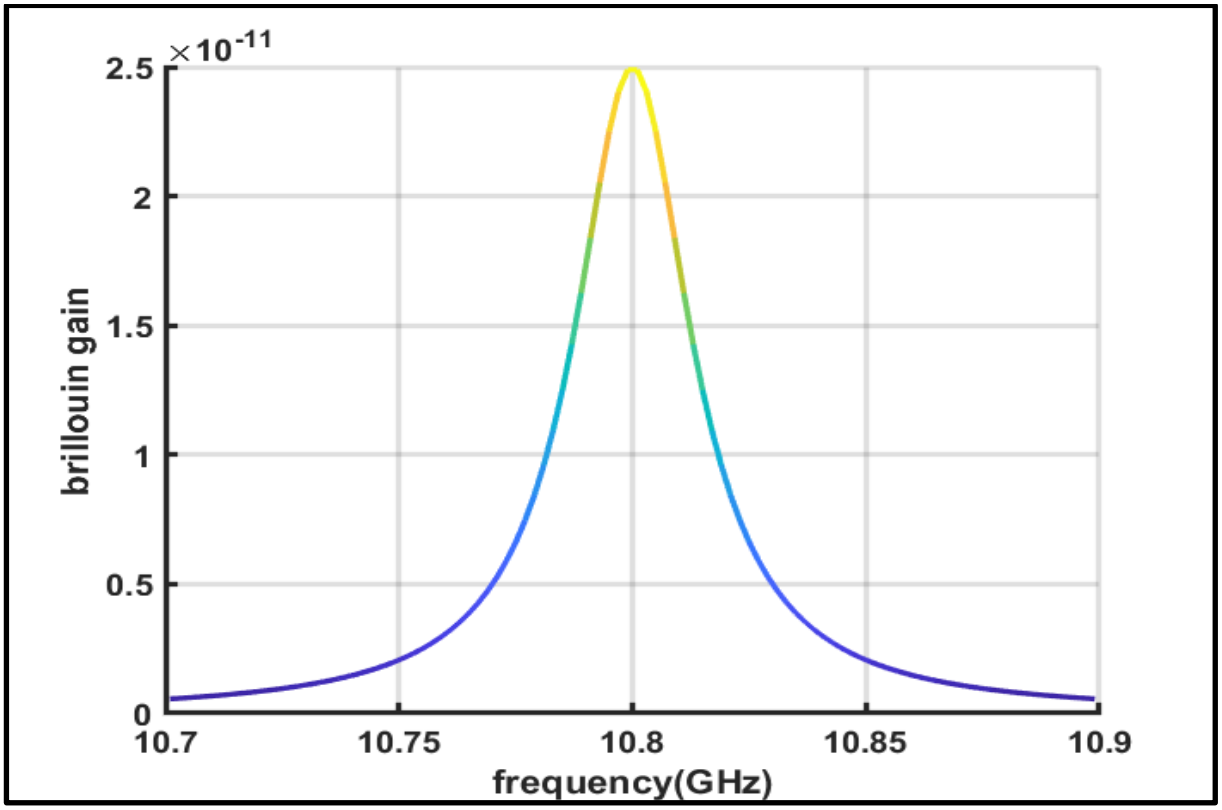

Fig.1.09: Natural Brillouin gain considering BFS to be 10.8 GHz

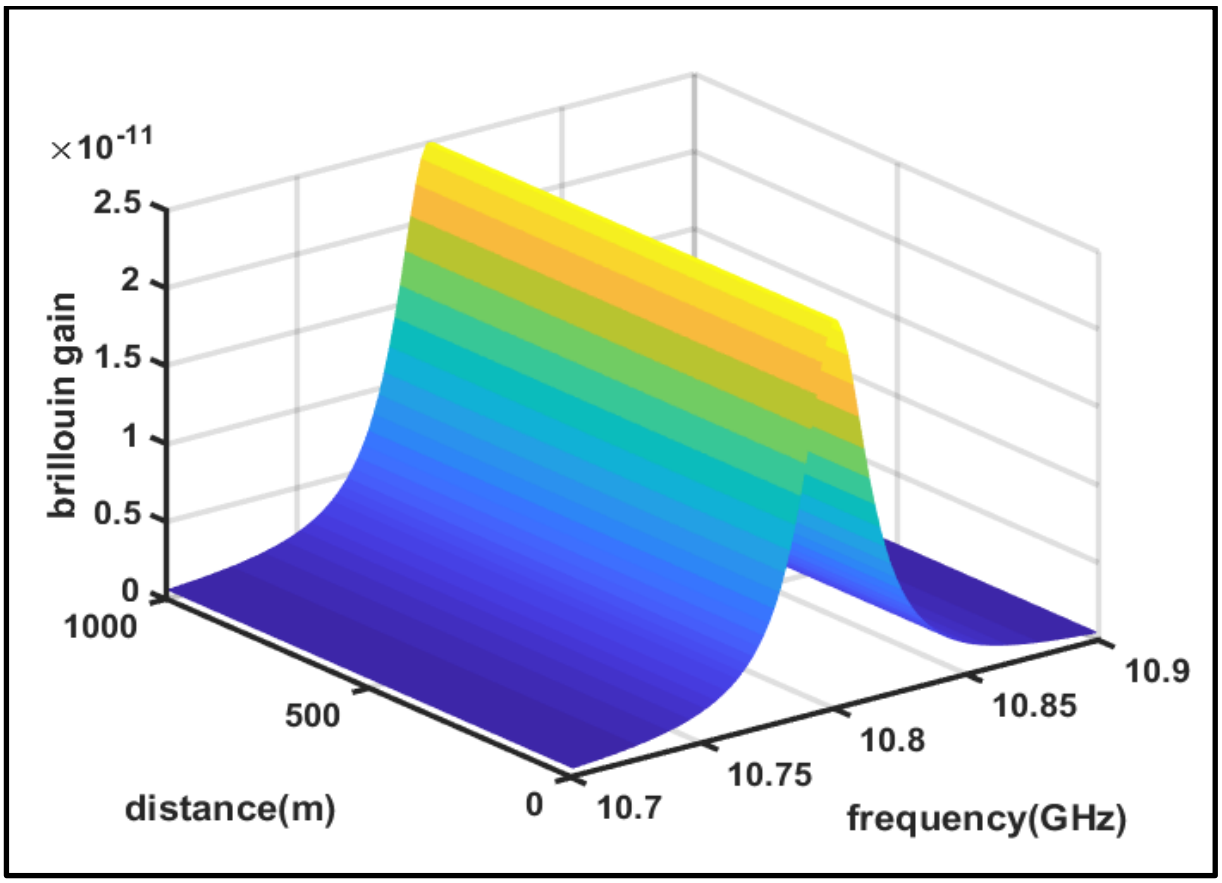

Fig.1.10: 3D plot showing Brillouin gain over distance

2. Stimulated Brillouin scattering in optical fibers

Stimulated Brillouin scattering (SBS) is a nonlinear process, which was experimentally evidenced in crystals by SBS process can occur in optical fibers at relatively low input-power levels, compared to other nonlinear effects, and it is a well-known obstruction in optical communications and high power fiber-optics lasers. The cause of the nonlinearity of the SBS process is the fact that the acoustic wave, whose power reflects the magnitude of the scattering process, is excited by the two light waves interference, through a phenomenon called electrostriction. The interference of the enhanced backscattered lightwave with the source lightwave enhances the acoustic wave through electrostriction and therefore this process is growing stronger along the fiber length.

2.2Electrostriction

Electrostriction is the tendency of materials to become compressed in the presence of an electric field. Electrostriction is of interest both as a mechanism leading to a third-order nonlinear optical response and as a coupling mechanism that leads to stimulated Brillouin scattering (Boyd 2007)

2.3 SBS and the electrostriction process

When two counter-propagating light waves meet, the interference of their electrical fields will excite an acoustic wave through electrostriction, if their frequency difference matches the properties of the optical fiber by fulfilling the conservation of momentum and energy, as expressed in Equations above. More accurately, the frequency difference between the two light waves may not be exactly tuned as required by these equations, and the SBS process will still occur. In this case, the efficiency is determined by the Brillouin spectrum and the frequency gap between the frequency difference and the BFS, as will be shown later.

The excited acoustic wave propagates at the speed of sound (~5500m/s in silica) in the same direction as the upper-frequency lightwave (UFL), causing a moving sine-shaped pattern of refractive index (a moving Bragg grating). This 'moving Bragg grating' backscatters a portion of the UFL with a down-shifted frequency, due to the Doppler Effect, which equals the frequency of the counter-propagating lightwave. In this way, energy is transferred from the UFL to the lower one. The lower frequency lightwave (LFL) can either be introduced to the fiber or generated through a spontaneous Brillouin scattering process.

If the process begins with a LFL much weaker than the UFL, amplification of the UFL by the SBS process causes enhancement of their interference and consequently enhancement of the acoustic wave. As a result, more energy is transferred from the UFL to the LFL and an iteratively growing process, shown in **Fig. 1.11** below.

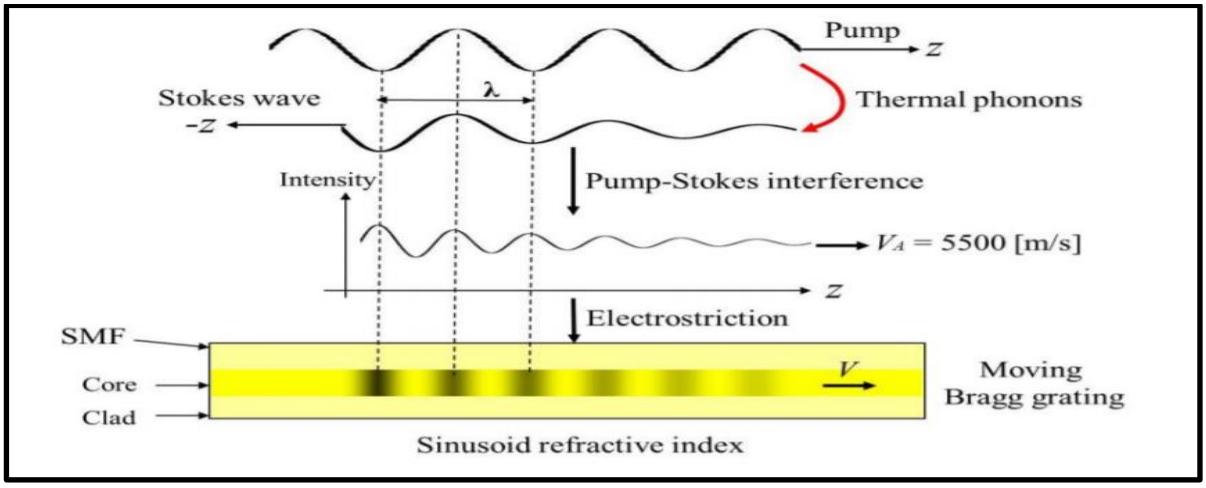

Fig.1.11: Stimulated Brillouin process, beginning from a pump wave, and its spontaneous Brillouin scattering. The Stokes wave is initially scattered by thermal phonons. As it is amplified, its interference with the pump wave is enhanced as well, and so is the Bragg grating along the –Z axis, in a iterative manner.

SBS is a gain process in which the pump power is transferred to the Stokes wavelength mediated through acoustic waves. Hence due to Brillouin scattering, part of the optical power launched into the fiber is backscattered as Stokes wave with 30 MHz bandwidth as shown in **Fig1.09.**

When the incident power exceeds certain value known as Brillouin threshold, the throughput power is found to saturate coinciding with an increase in the backscattered power. The threshold incident power for the onset of Brillouin scattering is given by

$$P_{th} = 21\frac{A_{eff}}{Leff\ g_o}$$

Where, A_{eff} is the effective mode area, L_{eff} is the effective nonlinear length of the fiber given by

$$L_{eff} = \frac{1-e^{-\alpha L}}{\alpha}$$

Where, $\alpha\ is$ the attenuation coefficient of optical fiber and L is is the length of the optical fiber.

This limits the amount of power that can be transmitted through an optical fiber. For, a 14 km fiber SBS threshold is found to be around 13.2 dBm, and for a 2 km fiber SBS threshold is around 17 dBm.

Although SBS has been a major factor limiting the performance of an optical communication system or a high power laser system, there are several applications which make use of Brillouin scattering phenomenon such as narrowband tunable filters , fiber sensors etc.

Sensing using Brillouin Scattering

When an optical fiber is subjected to perturbation like strain/temperature at specific locations, the density of medium changes at those locations because of which the acoustic velocity (V_a) changes. This leads to change in the local BFS which is proportional to the acoustic velocity. Hence, measurement of BFS along the fiber provides the information on the perturbation in the medium. As mentioned earlier, in order to detect any perturbation on a civil structure the optical fiber is bonded or embedded within the structure such that the perturbation is experienced by the optical fiber which leads to change in the local BFS.

In order to enhance the strength of the Brillouin scattered signal, another light wave referred to as probe which is downshifted in frequency from that of the pump by BFS is launched from the other end of the optical fiber. Different configurations have been implemented using the Brillouin scattering for sensing. These are Brillouin optical time domain reflectometry (BOTDR), Brillouin optical time domain analysis (BOTDA), Brillouin optical correlation domain analysis (BOCDA).

Brillouin Optical Time Domain Analysis

BOTDA is based on the SBS interaction between two counter-propagating light waves, referred to as pump and probe, in a sensing fiber. While their interaction, the pump wave, having a frequency higher than that of the probe wave, transfers energy to the probe wave, through a temporally-exited acoustic wave. It can also be interpreted as amplification of the probe by the pump.

BOTDA setup:

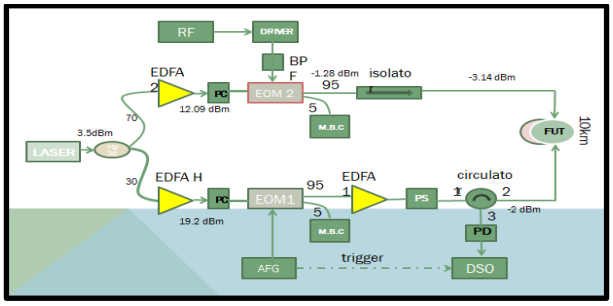

Fig.1.12: BOTDA for a 10 Km FUT

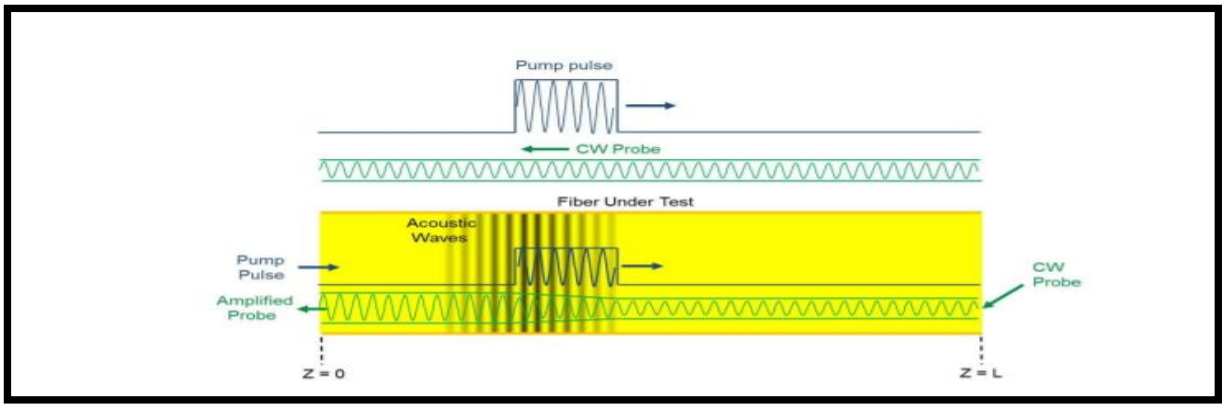

Fig.1.13: Illustration of BOTDA sensing process. The interaction between the pump pulse wave, the CW probe wave and the fiber medium excites a temporal acoustic wave, which leads to the amplification of the probe wave

Some results on temperature sensing using BOTDA technique for a 10 Km fiber spool:

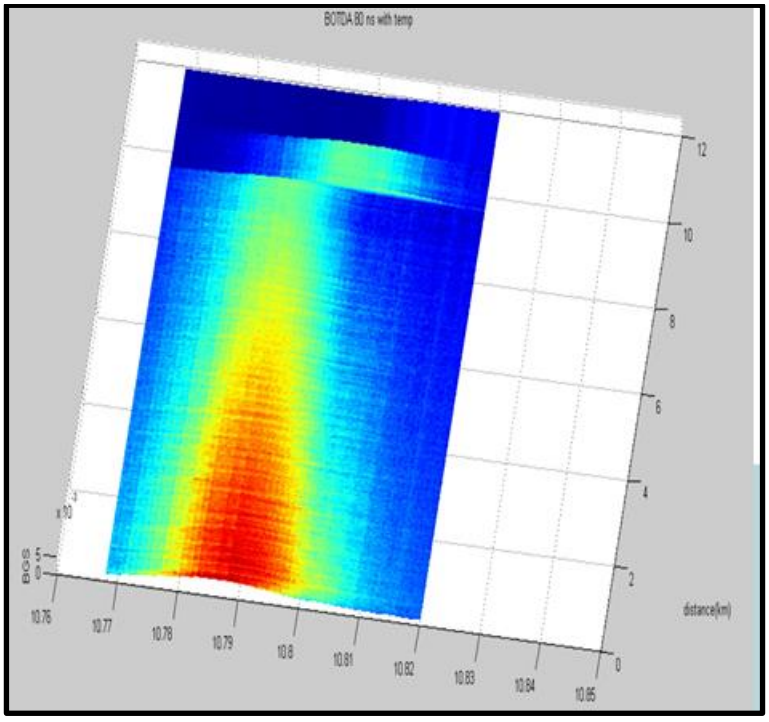

Fig.1.14: Temperature sensing using BOTDA technique on a 12 m section after a 10 km fiber

12m fiber from the existing 10 km spool was winded and kept on a hot plate then further connecting to a 1km spool. In AFG3252, pump pulses of width 80 ns are generated at a repetition rate of 120 µs which are intensity modulated on a round trip length of 10km (containing 12m portion) +1km fiber The RF is tuned from 10.7 GHz to 10.85 GHz. Total samples recorded is 100k @ 200MSa/sec, corresponding to 20 samples per pulse width, no of averages taken: 100

As the effective length of the SET fiber was found to be 9.75 km from previous BOTDA experiment, a temperature event is clearly noted after 9.75 km which corresponds to temperature applied over 12 m in hot plate .The actual change in BFS is noted by simultaneously plotting BFS of applied temperature vs. BFS of room temperature event and estimation of shift can be inferred by subtracting either .The subtracted trace (δBFS vs. distance) is also plotted).

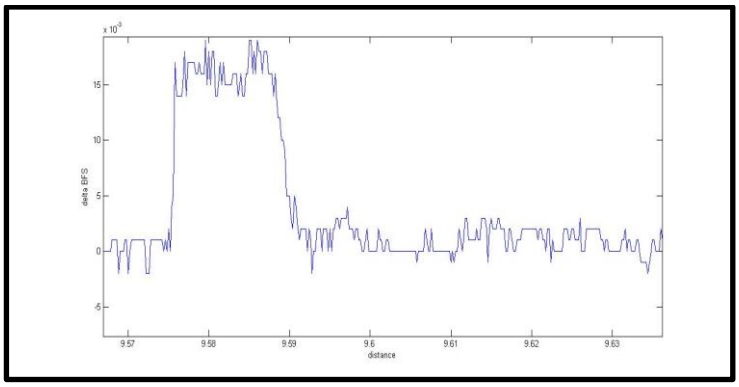

Fig.1.15: δBFS vs. distance

Fig.1.16 : Hot plate temperature

As can be seen from the zoomed plot in **Fig1.15**, maximum frequency shift noted 18MHz corresponding to distance (9.591km – 9.579 km) = 0.012 km i.e., 12 m (which is the actual distance over which strain is applied).Temperature coefficient for the fiber is 1.2MHz/°c thus indicating 21.6°c temperature shift while actual change in temperature noted is around 25 ° c. (47° c -22° c).

Limitations of BOTDA based sensors

The spatial resolution of the measurements in BOTDA is determined by the width of the pump pulse. In order to achieve good spatial resolution, one needs to use shorter pulse width for the pump light wave. However, this also results in lower SNR due to the shorter distance over which the Brillouin interaction takes place thereby reducing the measurement range. The SNR issue may be alleviated to a certain extent by employing averaging techniques at the expense of longer measurement time.

The spatial resolution problem in BOTDA is countered in correlation techniques like BOCDA where the SBS interaction is limited to “correlation peaks” or “sensing locations which is exclusively discussed in **CHAPTER 2**

Conclusions

This **CHAPTER** has dealt with the physics behind the Brillouin effect. It has been shown how the two counter propagating light waves, which are involved in the SBS process, are coupled by an acoustic wave through a phenomenon called electrostriction. And following it, temperature sensing using BOTDA technique is demonstrated and with it its limitation of spatial resolution is overcomed using a correlation based technique called BOCDA & investigated using a lock-in technique which are discussed in subsequent chapters.

PROJECT OBJECTIVE /GOALS:

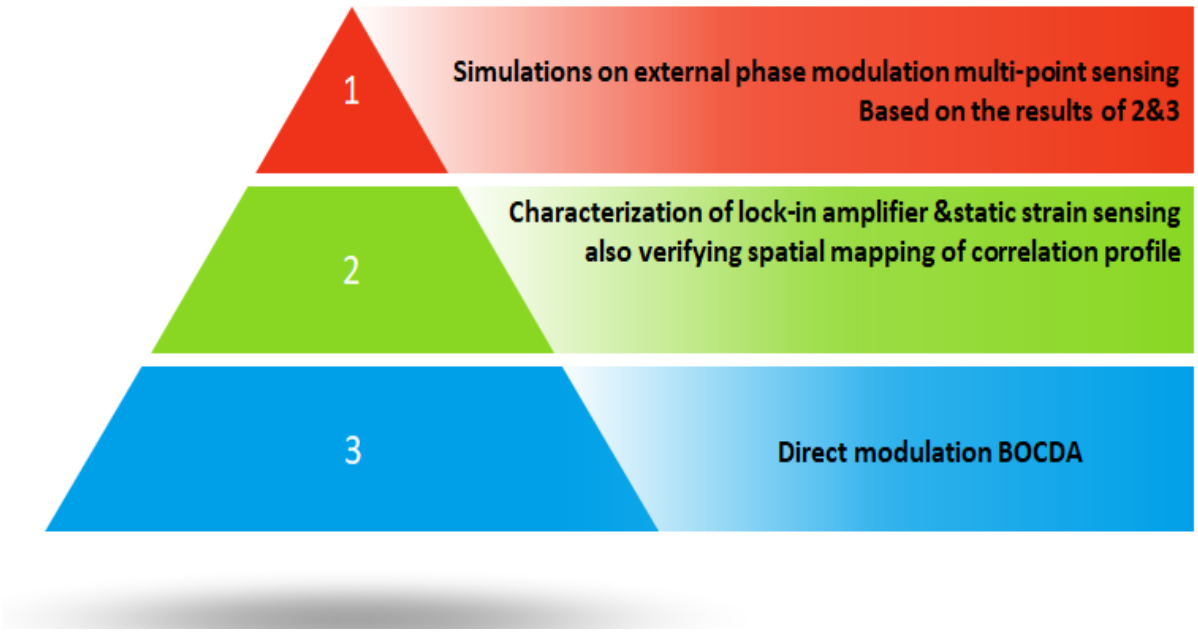

Chapter 2: BOCDA Technique

Details of BOCDA

Localization in SBS-based distributed sensing is achieved by spatially selective excitation of the acoustic field, a mission accomplished in BOTDA by the finite extent of the propagating pulsed pump. Too short pump pulses, however, successfully define the resolution cell but fail to allow the acoustic field to develop to its full strength and narrow (~30 MHz) spectral characteristics, resulting in a weaker and spectrally wider SBS interaction. It turns out that localization of the Brillouin interaction can also be achieved by judicious tailoring of the pump and probe waves to provide extremely high spatial resolution (down to millimetres) without compromising the width of the BGS.

Applications such as load monitoring of aircrafts require spatial resolution of the strain measurements in of the order of few centimetres. The spatial resolution limitation present in the BOTDA technique is overcome by using the BOCDA technique where the pump and the probe are frequency modulated thereby localizing the Brillouin interaction. Such localization of Brillouin process also provides an excellent opportunity for measuring dynamic strain or temperature variations at that location. The ability of frequency modulation of pump and probe to localise the Brillouin interaction is discussed in detail in this section. Unlike BOTDA wherein a pulsed pump radiation is used, the BOCDA technique uses continuous wave pump and probe light waves.

BOCDA with sinusoidal modulated pump and probe frequencies

In BOCDA both pump and probe are quasi-CW waves, whose frequencies are modulated with the same sine wave of frequency f_m. Usually, both waves originate from the same laser source, which is directly modulated by a sine-shape frequency modulation (FM), i.e. the wavelength of the laser output varies sinusoidally. In addition, the sine-shaped frequency of the probe wave is down-shifted (with respect to the pump frequency), with a frequency shift to be tuned close to the BFS of the tested fiber. When the pump and probe waves are counter propagating, with their sine-shaped frequency modulation, their frequency difference acquires the form of a standing wave as shown in the figure below. Therefore, at each point along the fiber, except for a few node points of this 'standing wave', the pump-probe frequency difference varies much more rapidly than the time required for the build-up of the Brillouin acoustic wave (the phonon lifetime). Thus, only at the few node-points, which have a constant pump-probe frequency difference (i.e. where the pump and probe are correlated), is the acoustic wave excited, providing Brillouin gain to the probe wave. With a correct selection of the modulation frequency, f_m, and the delay in one of the branches, it can be guaranteed that only a single node-point will appear in the range of the sensing fiber. The location of the node-point along the fiber length is determined by fine-tuning the modulation frequency, f_m. With a single Brillouin-gain point, the properties

(temperature or strain) of this point can be obtained by mapping its local BGS; this is achieved by scanning the constant frequency-shift of the probe wave. In this way, the entire fiber can be interrogated along its length, point after point.

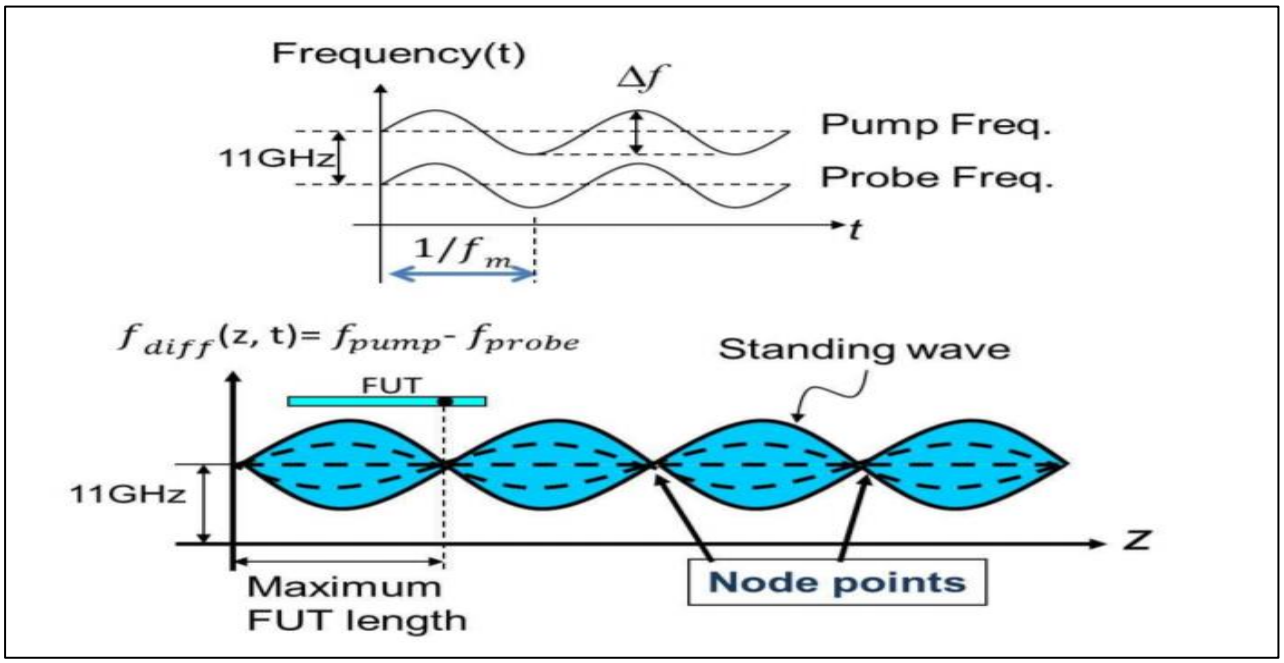

FIG2.01: The pump-probe frequency difference, f_{diff}, acts like a standing wave with some static node points, undergoing Brillouin amplification. One such node-point is used for sensing.

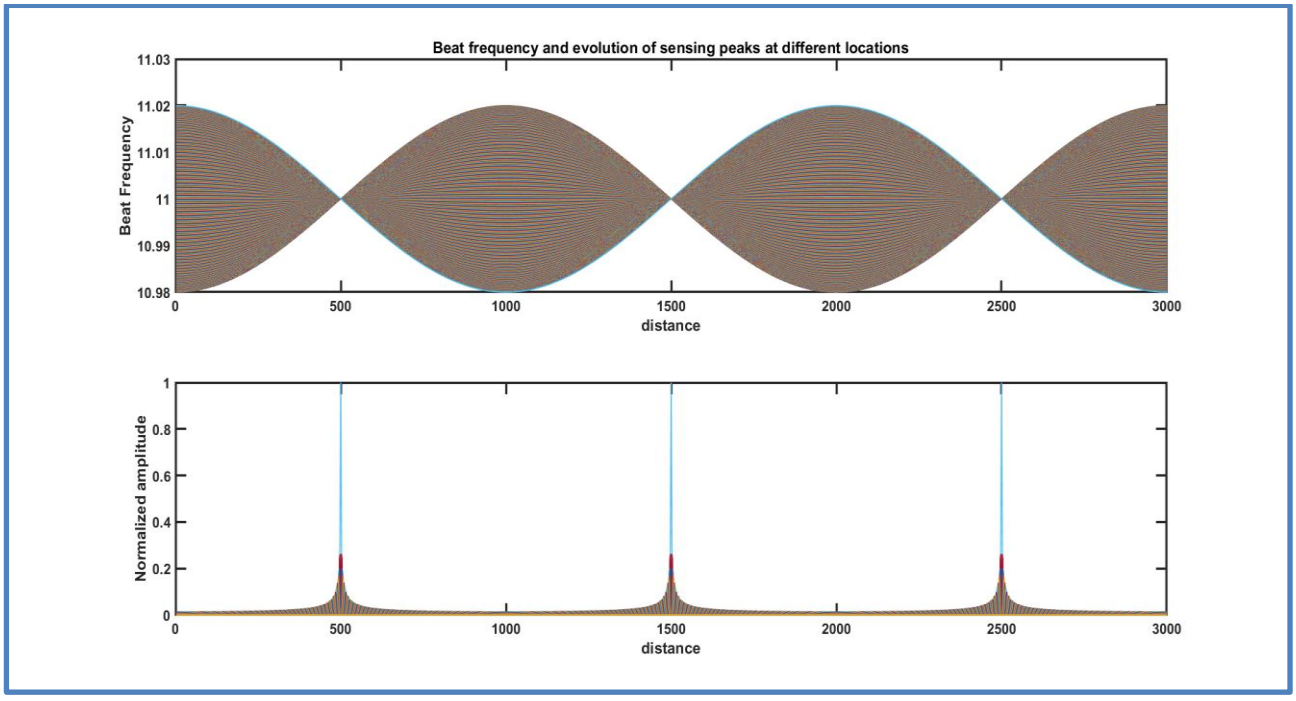

Fig.2.02 : Evolution of beat spectrum ('sensing locations') with f_{diff} =11GHz

Mathematical approach:

$E_{pump}= A_{pump} \exp [j(k_{pump}z – 2\pi(f_{pump} + \Delta f \cos(2\pi f_m(t-z/V_g))t))]$

$E_{probe}= A_{probe} \exp [j(-k_{probe}z – 2\pi(f_{probe} + \Delta f \cos(2\pi f_m(t-(l-z)/V_g))t))]$

At point z along the fiber the instantaneous frequency difference between these two waves is:

$f_{diff}(z,t) = f_{pump} - f_{probe} + \Delta f \cos(2\pi f_m(t-z/V_g)) - \Delta f \cos(2\pi f_m(t-(l-z)/V_g))$

$= f_{pump} - f_{probe} -2\Delta f \sin(\pi f_m (l-2z/V_g)) \sin(\pi f_m(2t-l/V_g))$

Interestingly, at those locations obeying:

$z_k = 0.5(l - k\frac{V_g}{f_m}), k = 0, \pm1, \pm2, \ldots$. The Δf term is zero and f_{diff} (Z_k, t) has a time-independent value of f_{diff} = fpump − fprobe, as if the fiber were interrogated by CW waves.

Thus, the BFS at any of these $\{z_k\}$ can be simply obtained by scanning f_{diff} = fpump − fprobe over the appropriate frequency range and then looking for the location of the peak of the measured BGS. Note that when f_{diff} assumes the value of the local BFS, $f_B(z)$,here 11GHz, a complete and stable build-up of the acoustic field is guaranteed. Also, the width of the measured BGS should ideally be as narrow as obtained from a CW interrogation. However, as z departs from the correlation peaks ,the Δf term is no longer zero, and the efficiency of the acoustic field build up quickly deteriorates since f(z, t) differs from the local BFS, f_B (z), even when fpump − fprobe = f_B (z). The spatial resolution of this method, Δz, is expected to be related to the BGS linewidth, $\Delta\nu_B$, since there is no appreciable build-up of the acoustic field once the pump-probe frequency difference exceeds $\Delta\nu_B$. Indeed, it has been shown that

$$\Delta z = \frac{c\Delta\nu_B}{2n\pi f_m \Delta z} = \frac{v_g \Delta\nu_B}{2\pi f_m \Delta z}$$

Note that the distance between two adjacent correlation peaks corresponds to d which is quantified using

$$d = \frac{c}{2nf_m} = \frac{V_g}{2f_m}$$

Correlation peaks:

The instantaneous beat frequency due to the beating of the pump and probe light waves varies around a mean of 11 GHz along the length of the sensing fiber. Clearly, the Brillouin interaction occurs only when the instantaneous beat frequency corresponds to 11 GHz. Beat frequency changes value over time all across the sensing fiber except for specific locations

where it remains constant at 11 GHz. The resultant Brillouin gain builds up consistently only at those locations commonly referred to as correlation peaks

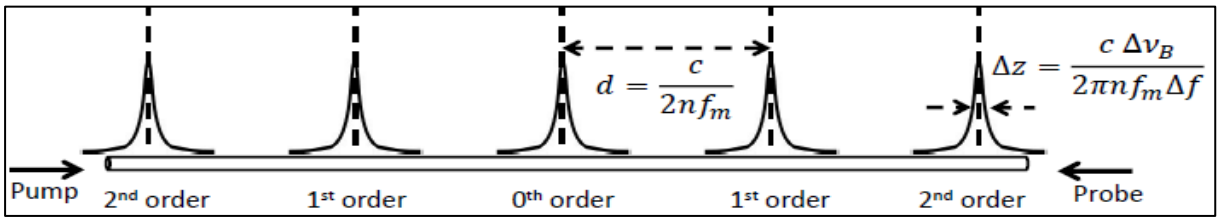

Fig2.03: correlation peaks generated within the FUT. If the pump and probe arm lengths are equal we will observe a correlation peak at the centre of the FUT. If the FUT is longer than 2d, we will observe more peaks on either side of the central peak.

Case 1: l<2d

l= 1.5km , fm =100 kHz (d= 1 km)

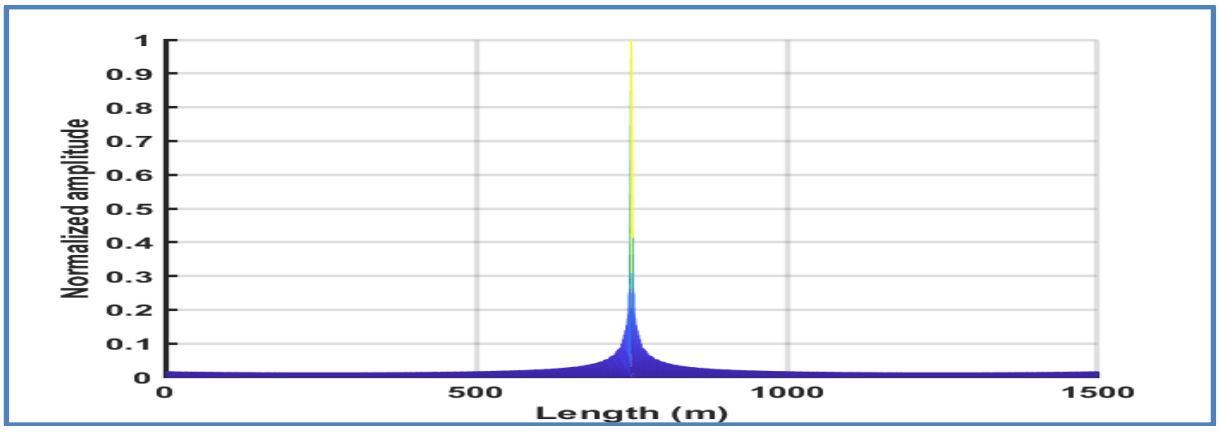

Fig2.04: only 1 correlation peak formed at 750 m

Case 2: l>2d

l=3km, fm =100kHz (d=1km)

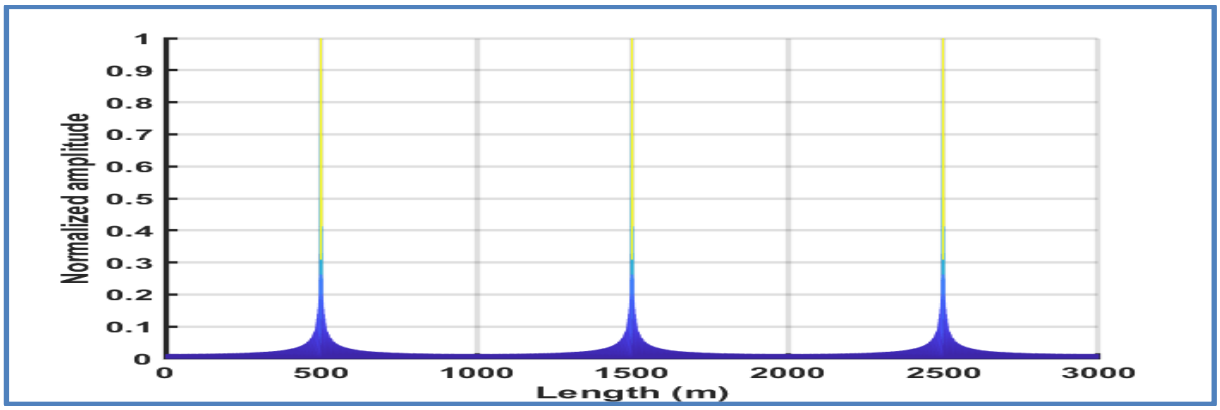

Fig2.05: 3 correlation peaks formed at 500m, 1500 m and 2500 m

Dependence of correlation peak on f_m (Distributed sensing)

For distributed sensing applications, we need to scan the correlation peak position across the sensing fiber. This may be achieved in BOCDA by changing the modulation Frequency, as explained below

$z_k = 0.5(l - k\frac{V_g}{f_m}), k = 0, \pm 1, \pm 2, \ldots$

As can be noted from the equation, varying f_m varies the correlation peak position except zeroth order. Now f_m is halved (50 kHz) , the higher order correlation peaks are swept away from the fiber .only the zeroth order peak is formed at the centre.

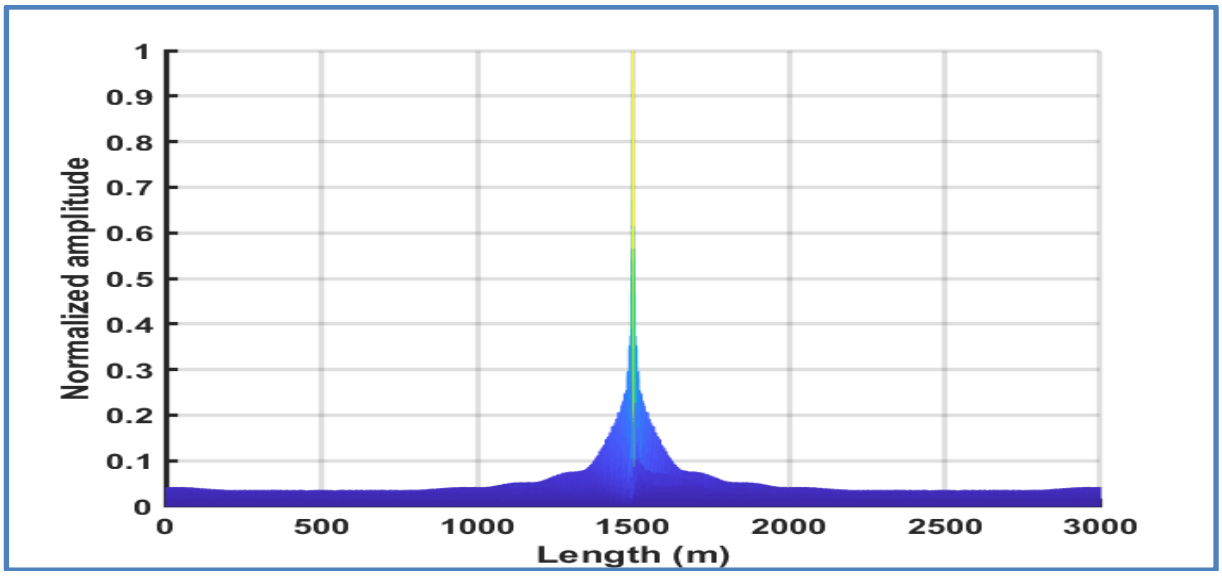

Fig 2.06: zeroth order correlation peak formed at 1500 m

Moving zeroth order correlation peak (incorporating a delay fiber)

Incorporating, delay fiber of 1Km, l= 3km , fm =50 kHz (d=2km)

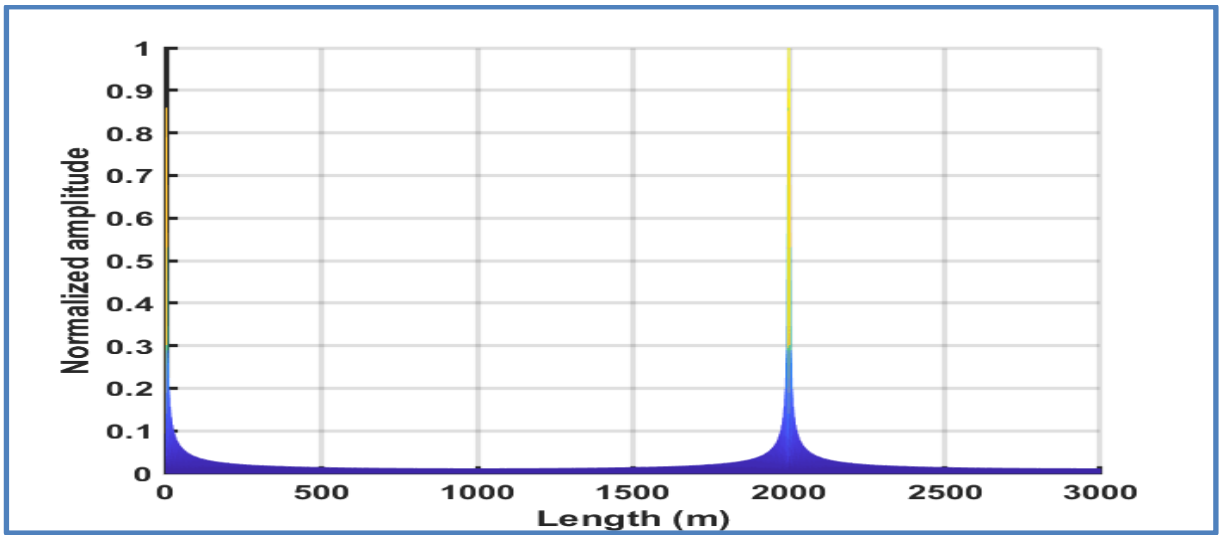

Fig 2.07: shift in zeroth order correlation peak

Spatial mapping of correlation profile (Simulations):

Brillouin Optical Correlation Domain Analysis (BOCDA) technique is helpful in localizing the Brillouin interaction with very high spatial resolution (1 cm) and is also very useful for detection of perturbations which are varying in a dynamic fashion. In this Chapter, the implementation and analysis of the BOCDA technique is discussed. The spatial mapping of Brillouin gain profile in the sensing fiber, which is critical in identifying the sensing location is investigated through simulations and verified through controlled experiments.(*excerpts of the code are taken from somepalli bhargav's thesis)

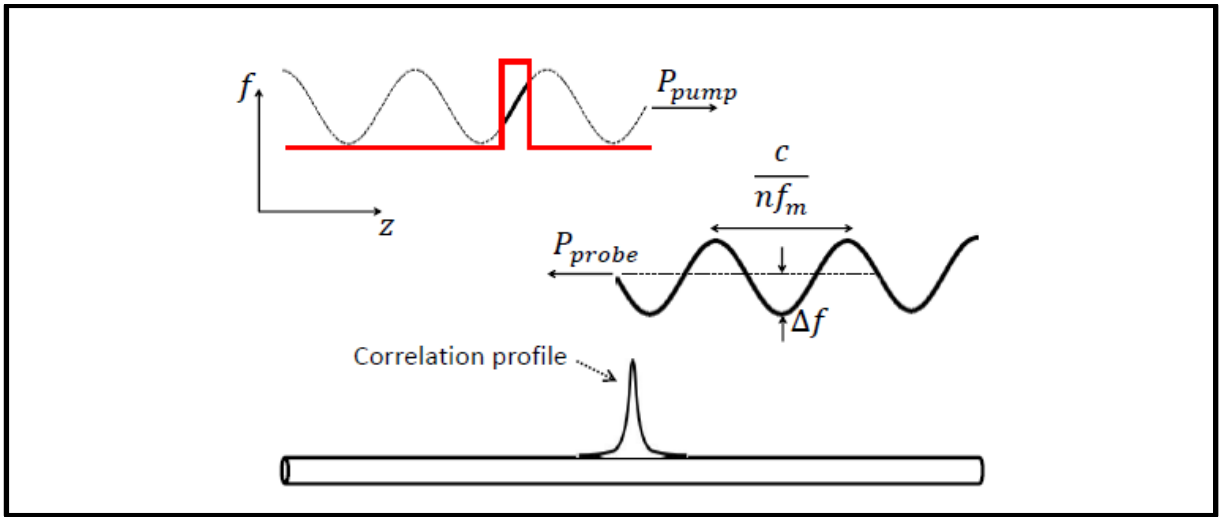

Fig 2.08: Interaction of pulsed pump and CW probe in BOCDA for spatial mapping of correlation profile.

As shown in the above figure, the pump and the probe are frequency modulated with a modulation frequency f_m and frequency deviation Δf. In order to spatially map the correlation profile along the fiber under test, the pump is further intensity modulated with a train of pulses with pulse widths much smaller than the period of frequency modulation.

MATHEMATICAL MODELLING:

In order to numerically model the BOCDA system, SBS interaction between pump and probe is considered using steady-state equations [Boyd (2008)]. Under un-depleted pump approximation and neglecting fiber losses, the probe power can be expressed as:

$$P_{probe}(z,t) = P_{probe}(z+dz, t-dt) exp(g_B(z,t) \frac{P_{pump}(z,t)}{A_{eff}} dz)$$

$$g_B(z,t) = \frac{g_o}{1+ \left(\frac{\left(f_{B-} fdiff(z,t)\right)}{\Delta \nu_B / 2}\right)2}$$

$$f_{pump(z,t)} = f_c + \Delta f \sin\left(2\pi f_m\left(t - \frac{z}{V_g}\right)\right)$$

$$f_{probe(z,t)} = f_c - f_B + \Delta f \sin\left(2\pi f_m(t - \frac{l-z}{V_g})\right)$$

Where,

dz = space step size

dt = time step size

P_{probe} = instantaneous probe power

P_{pump} = instantaneous pump power which is a train of pulses

g_B = SBS gain factor

A_{eff} = effective area of the fiber

g_o = peak Brillouin gain

f_B = Brillouin Frequency Shift

$\Delta \nu_B$ = Brillouin gain bandwidth

$f_{diff\ (z,t)}$ = Beat frequency between pump and probe at specific z & t .

$f_{pump(z,t)}$ = instantaneous frequency of pump at any location z

$f_{probe(z,t)}$ = instantaneous frequency of probe at any location z

f_c = optical carrier frequency

Δf = frequency deviation

f_m = modulation frequency

l = length of the fiber

V_g = group velocity of light in fiber

The MATLAB code used to simulate the spatial mapping of correlation profile in BOCDA is given in Appendix A.*

Results :

Spatial Mapping of Zeroth order correlation peak in 2Km fiber

Parameters : f_m = 10KHz , l = 2.2 km , Δf =0.532 GHz ,

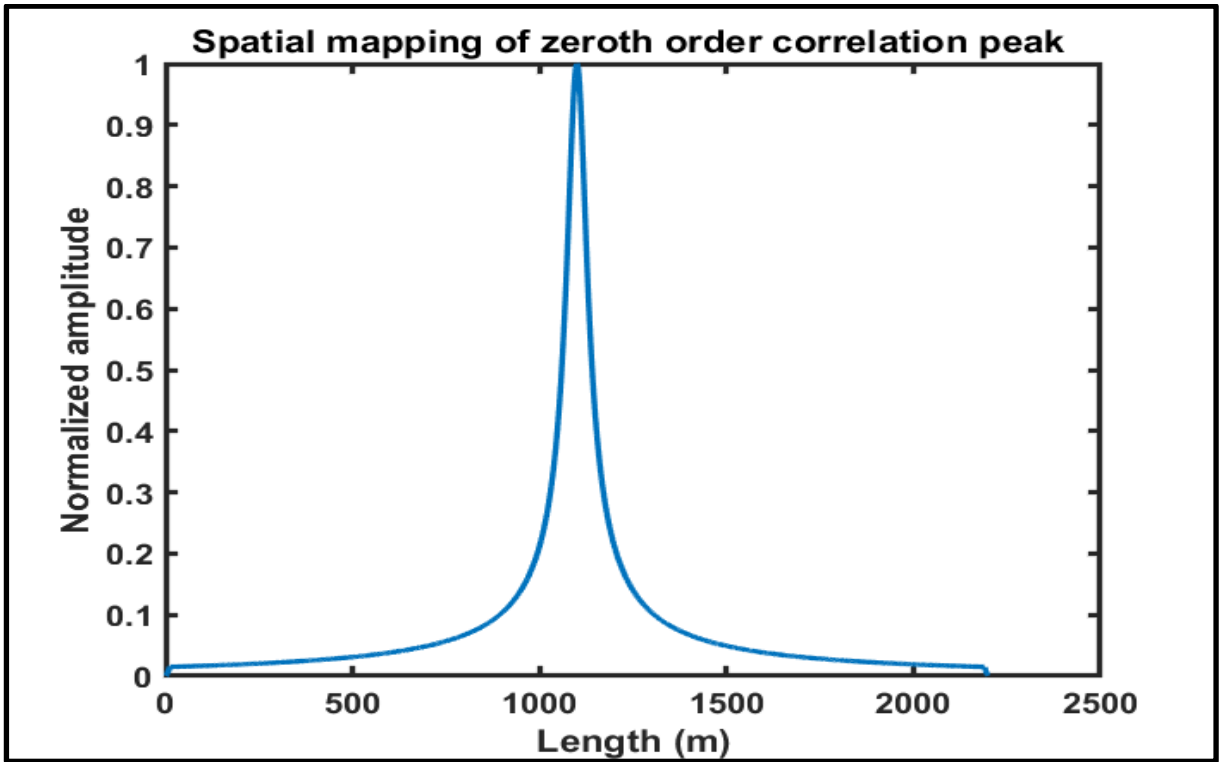

Fig 2.09: zeroth order correlation peak formed at 1.09 km

Due to the use of pulsed pump for spatially mapping the correlation profile, the spatial mapping technique suffers from the phonon lifetime limit (similar to BOTDA technique) and hence the accuracy of the spatial mapping of correlation profile is not better than 1 m.

The correlation profile obtained through simulations with an f_m of 10 kHz, Δf of 0.532 GHz and pump pulse width of 200 ns is shown in the figure. Correlation peak is observed at around 1.09 Km where Brillouin gain is maximum.

EXTERNAL PHASE MODULATION BOCDA (SIMULTANEOUS MULTI-STRAIN MONITORING)

In order, to monitor multiple locations simultaneously, multiple correlation peaks have to be generated within the FUT. So, multiple correlation peaks (sensing locations) should have different f_m (say f_{m1} , f_{m2} , ……) so that after lock-in detection at f_{m1} , f_{m2} , ……those signatures are recovered simultaneously.

The required sinusoidal FM signals with unique sets of f_m & Δf are generated in electrical domain & these locations are transferred to optical domain through external phase modulator (PM).

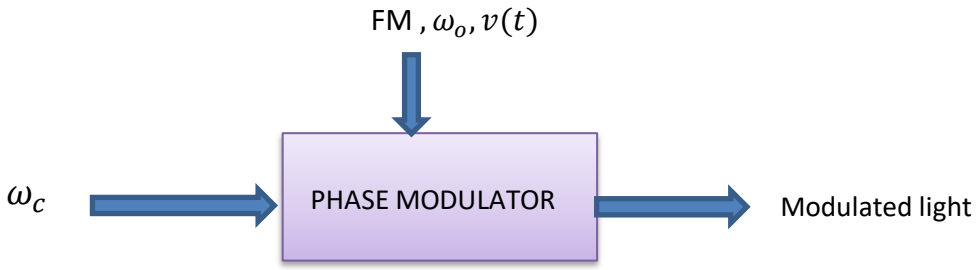

Where , ω_c = light carrier frequency

ω_o = center frequency of FM

$$v(t) = V_{o1}\sin\{\omega_{o1} + \beta_1\sin(2\pi f m_1 t)\} + V_{o2}\sin\{\omega_{o2} + \beta_2\sin(2\pi f m_2 t)\}$$

$$E_{mod}(t) = E_o\, exp(jw_c t)\, exp(j(\frac{\pi\, v(t)}{v_\pi}))$$

$$E_{mod}(t) = E_o\, exp(jw_c t) + E_1 exp\left\{ j((w_c + w_o)t + \frac{\Delta f}{f_m}\sin(2\pi f_m t)\right\} - E_1 exp\left\{ j((w_c - w_o)t - \frac{\Delta f}{f_m}\sin(2\pi f_m t)\right\}$$

Spectrum of $v(t)$

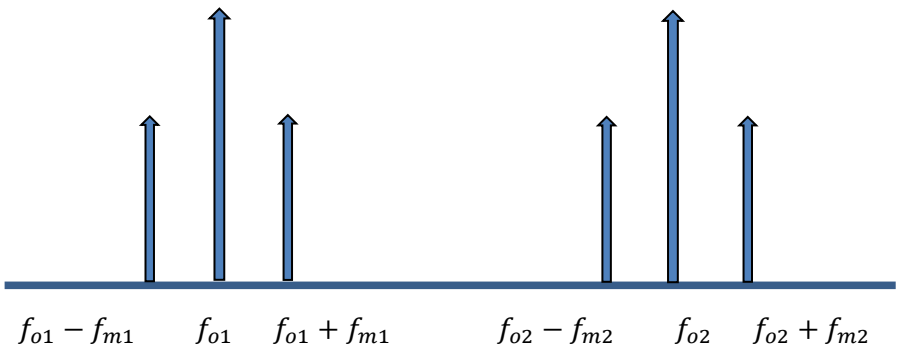

Spectrum of phase modulator output :

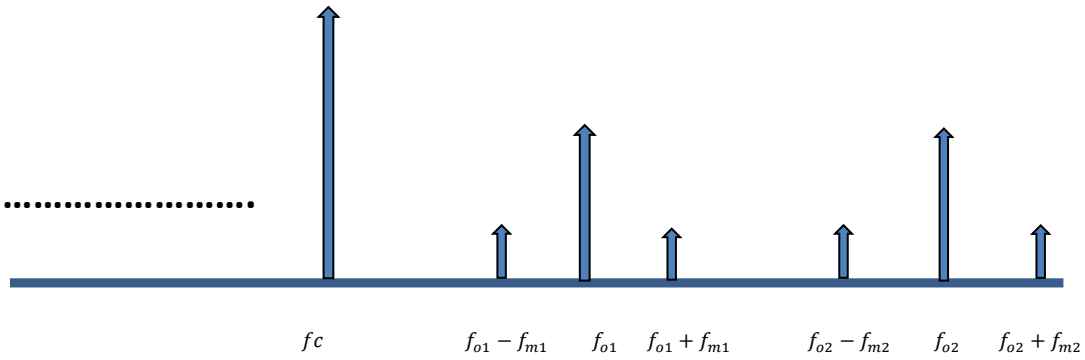

MULTI-POINT SENSINGSIMULATION RESULTS:

Center frequency of FM 1, f_{c1} = 6 GHz

Modulation frequency, f_{m1} = 60 kHz

Frequency deviation, Δf_1 = 0.5 GHz

Center frequency of FM 2, f_{c2} = 6GHz

Modulation frequency, f_{m2} = 71 kHz

Frequency deviation, Δf_2 = 0.5 GHz

Sampling time = 5ns

Length of sensing fiber = 1 km

Length of delay fiber = 13.4 Km

Note :

1. O^{th} order correlation peak will be formed at 7.2km (1km_FUT+13.4km _delay _fiber)
2. For f_{m1}=61 kHz, d= 1.639 Km
3. For f_{m2}=70 kHz, d= 1.428 Km
4. So , 4^{th} order correlation peak will be formed for 61 KHz component at position (7.2-(4*1.639)) km = 643 m from start of fiber.(pump end)
5. And 5^{th} order correlation peak will be formed for 70 KHz component at position (7.2-(5*1.428)) km = 60 m from start of fiber. (Pump end)

Case 1: strain corresponding to BFS shift of 10MHz applied at location corresponding to 61 kHz and lock-in at 122 kHz while other location is unstrained

Case2: strain corresponding to BFS shift of 10MHz applied at location corresponding to 61kHz and lock-in at 140kHz while other location is unstrained

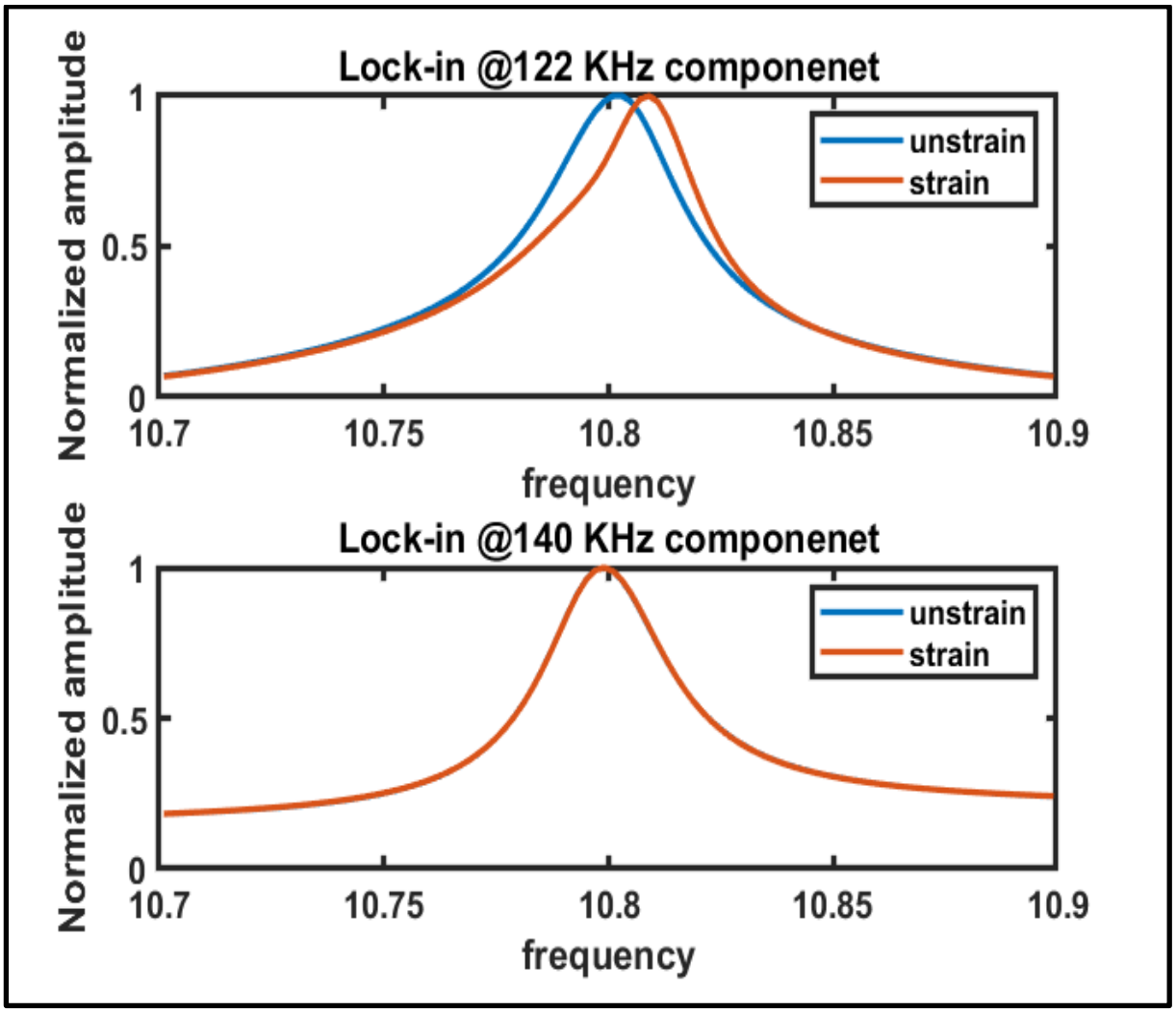

Fig2.10: corresponding BGS plot

Case 3: strain corresponding to BFS shift of 10MHz applied at location corresponding to 70kHz and lock-in at 140kHz while other location is unstrained

Case4: strain corresponding to BFS shift of 10MHz applied at location corresponding to 70kHz and lock-in at 122kHz while other location is unstrained

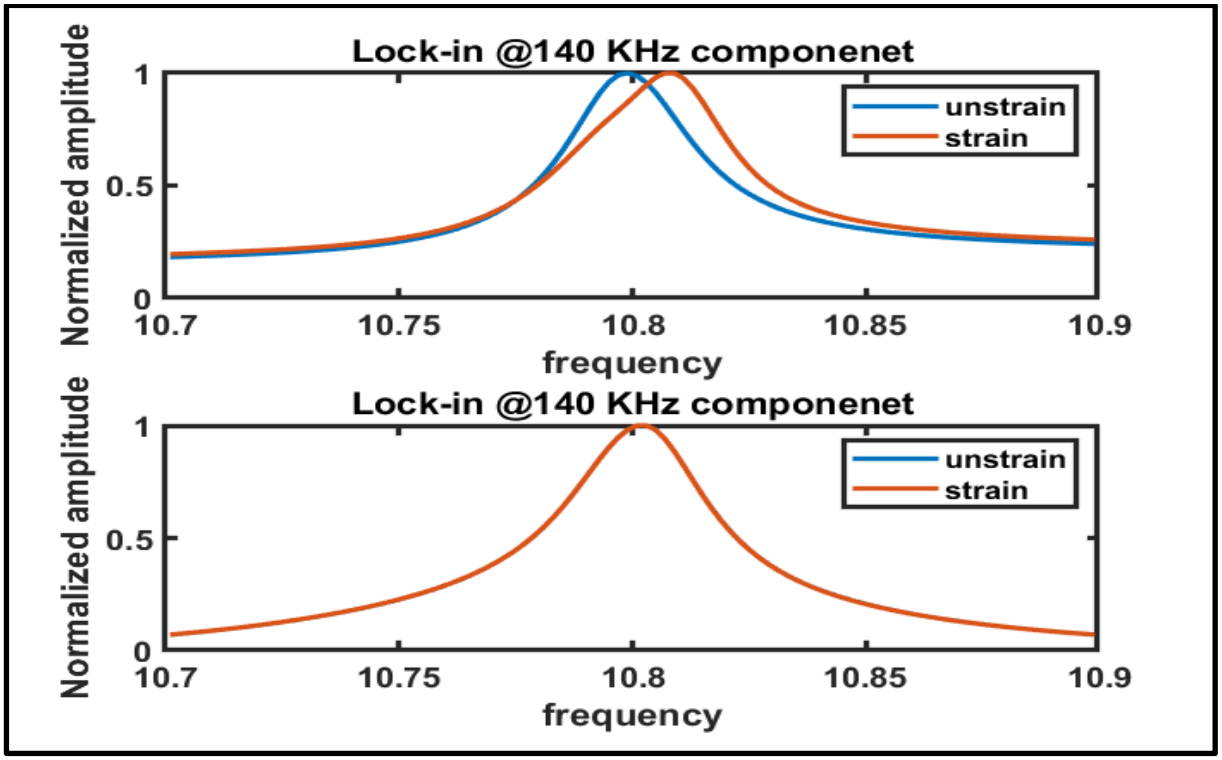

Fig2.11: corresponding BGS plot

Case 5: different strain magnitude @10MHz shift in BFS corresponding to 61 kHz and lock-in at 122 kHz & strain magnitude @20MHz shift in BFS corresponding to 70 kHz and lock-in at 140 kHz

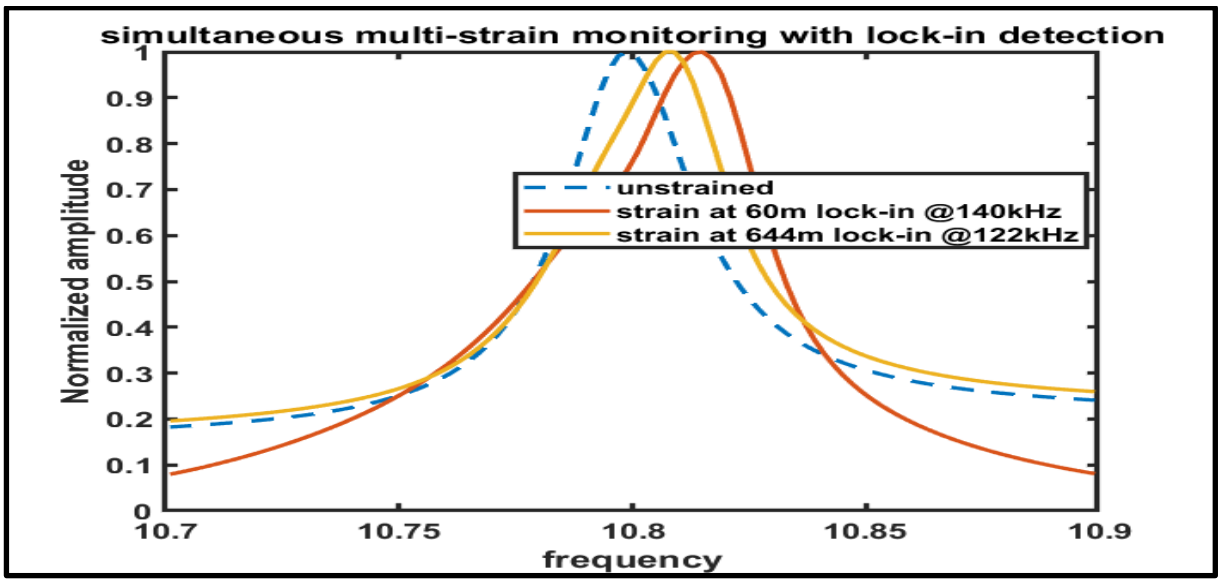

Fig2.22: corresponding BGS plot

*excerpts of the code are taken from somepalli Bhargav's thesis) as a proof of principle

CHAPTER 3 (BOCDA EXPERIMENTS)

Schematic of classical BOCDA (direct modulation)

A schematic diagram of the experimental setup used in the BOCDA based sensors is shown in **Fig.3.01** .The frequency modulation (FM) of pump and probe is achieved typically by appropriately modulating the current driving the laser. When the input current to the laser is modulated, it results in a change in the carrier density and hence modulates the refractive index of the laser gain medium. This results in a corresponding change in the instantaneous frequency of the laser. The frequency modulated laser output is split into pump and probe light waves. The pump light wave is amplified and is launched into the FUT after polarization scrambling. The probe is frequency shifted and is launched into the other end of the FUT. The frequency modulated pump and probe interact in the FUT such that the Brillouin interaction occurs only at specific locations referred to as correlation peaks. The location of correlation regions is periodic due to the periodic nature of the FM modulation.

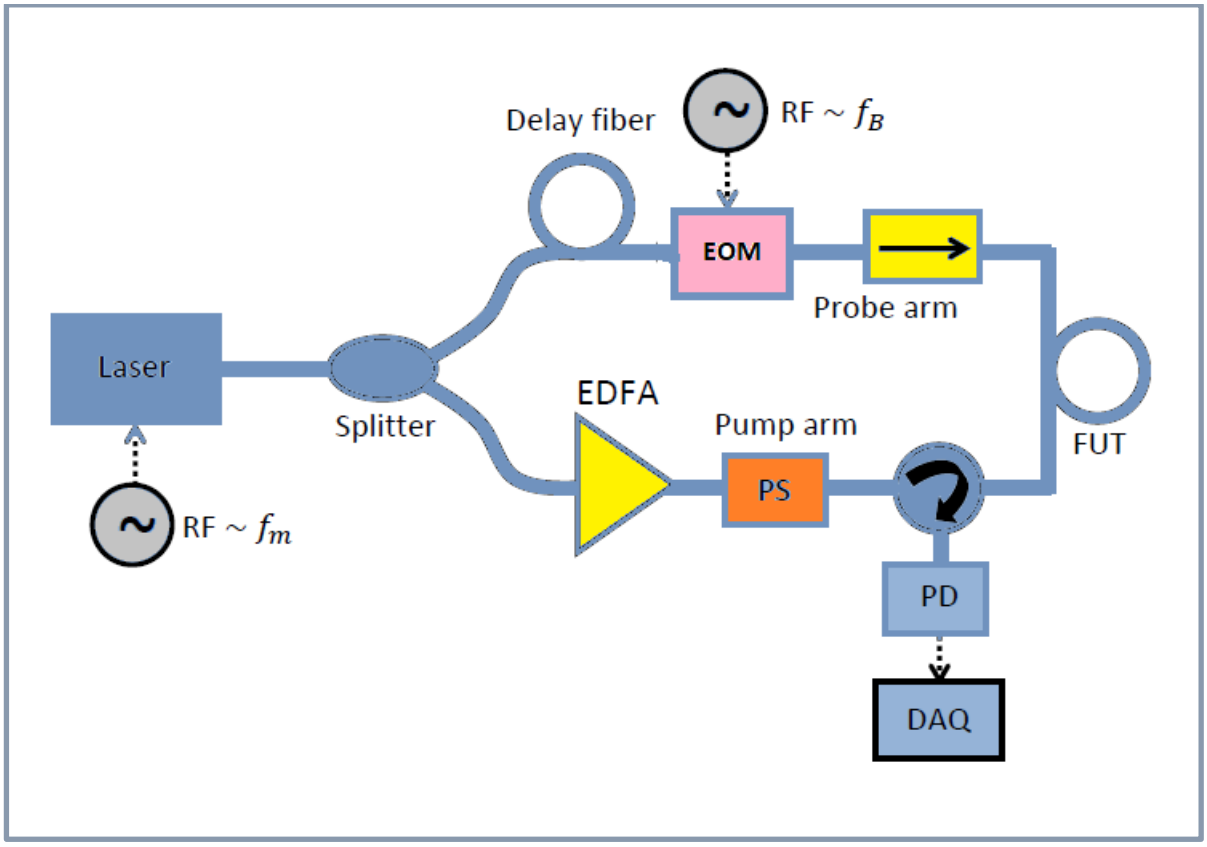

Fig.3.01 BOCDA experimental setup

Spatial Mapping:

Spatial mapping of the 0th order correlation peak in a 2km long fiber is experimentally demonstrated using direct modulation of laser & dependence of spatial resolution on the maximum frequency deviation is also shown:

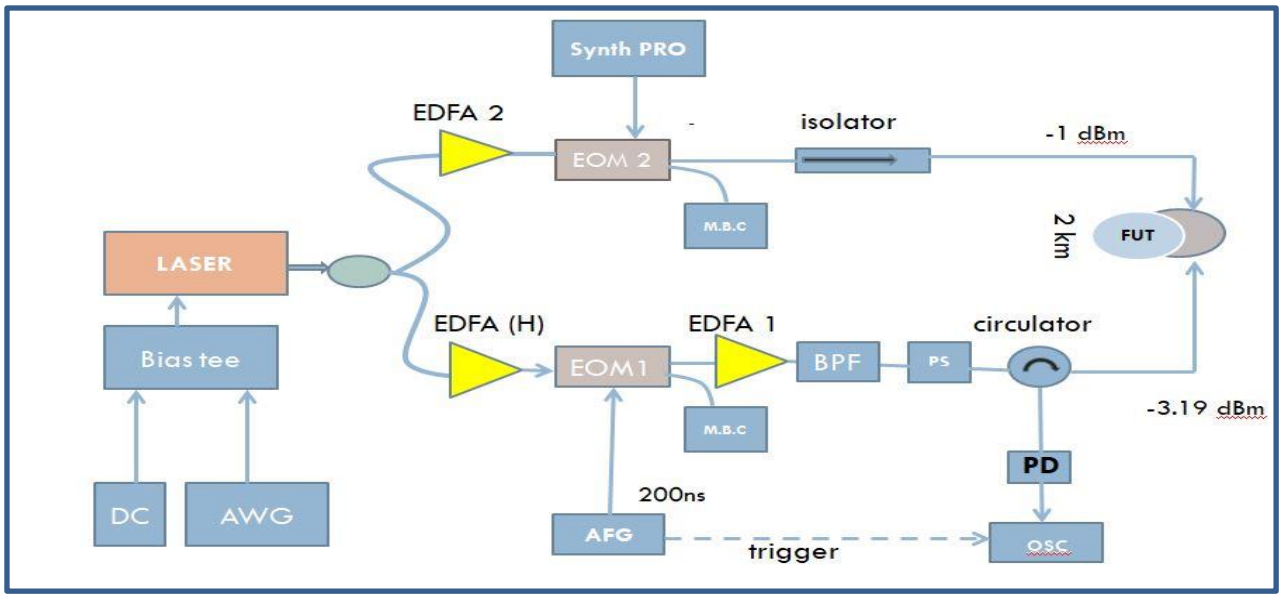

Fig.3.02 Spatial mapping experimental setup

The Laser used for the experiment is an Eblana Laser at wavelength of 1559 nm, having line width of 2 MHz .The laser is directly modulated by modulating the driving current using an AWG. The bias point is fixed at 4.2V.The light is then split into two arms to generate the pump and the probe light waves. The pump arm is intensity modulated to generate pulses with pulse widths of 200 ns at a repetition rate of 25 µs, corresponding to the round-trip time of the 2km long FUT. The BFS of the 2km fiber is estimated through BOTDA at 10.771 GHz. The probe is frequency shifted with respect to the pump at the BFS itself.

The specifications used for the experimental setup are thus:

f_m= Modulation frequency of pump/probe= **10 kHz**, corresponding to a dynamic range of 10 km.

Length of fiber chosen is= **2.18 km** (exact length estimated through BOTDA measurement)
No. of averages taken= **200**
BFS of the fiber estimated through BOTDA= **10.771 GHz**

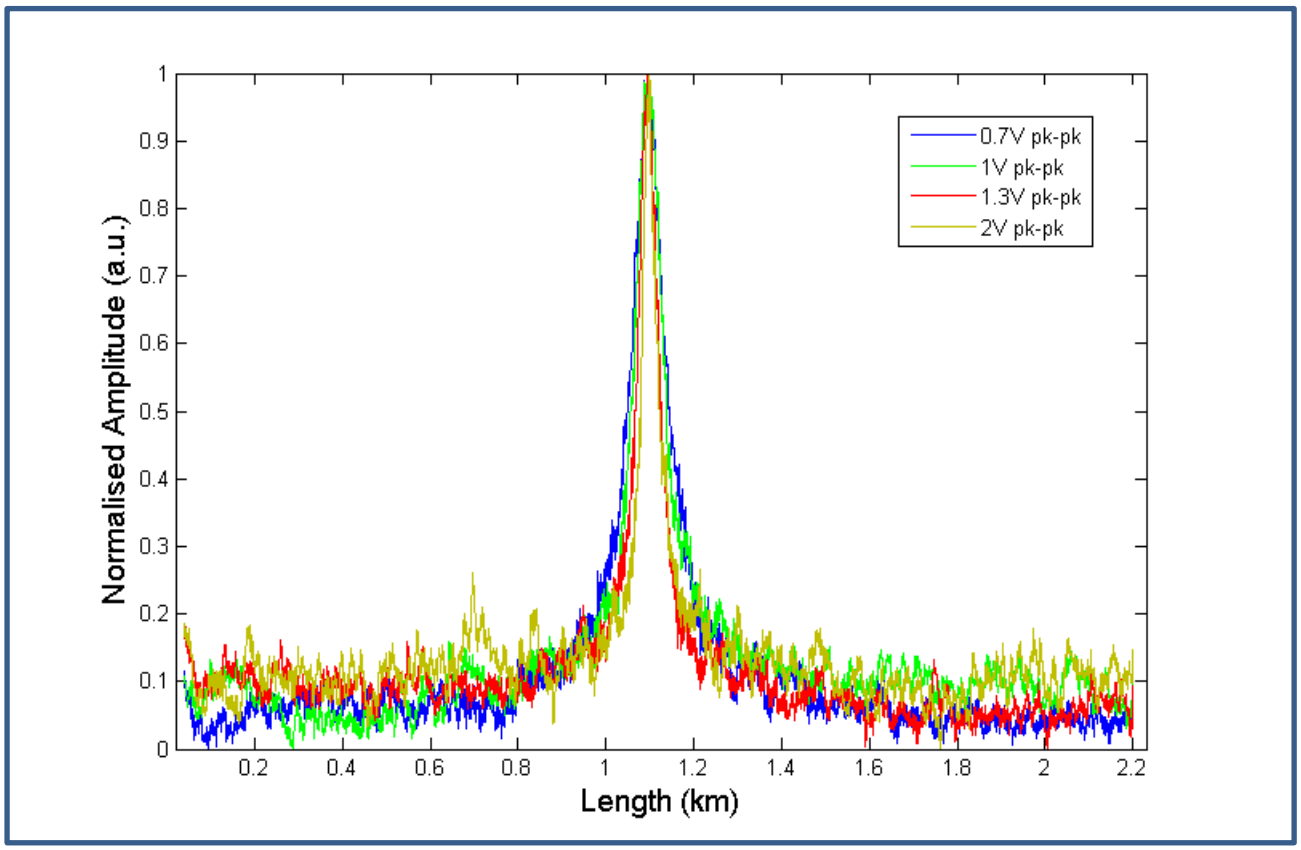

Fig.3.03 Spatial mapping of 0th order correlation peak for varying peak-to-peak voltages, f_m= 10 kHz, pulse width=200 ns

We know that for direct modulation, as the current swing increases, the frequency deviation is also expected to increase. Also, as Δf increases, we can expect the spatial resolution Δz to decrease as per the equation provided below. **Fig.3.03** shows the spatially mapped 0th order correlation peak for different peak-to-peak values of applied sinusoidal signal.

$$\Delta z = \frac{c\,\Delta v B}{2\pi n f m\,\Delta f}$$

The zeroth order correlation peak is obtained near the center of the FUT. Thus, it is concluded that the optical path lengths of the pump and probe arms are almost equal since zeroth order correlation peak occurs where the two paths are equal.

It is also experimentally verified that the width of correlation peak /spatial resolution is dependent on the amount of frequency deviation. As frequency deviation increases, the width is found to decrease as expected.

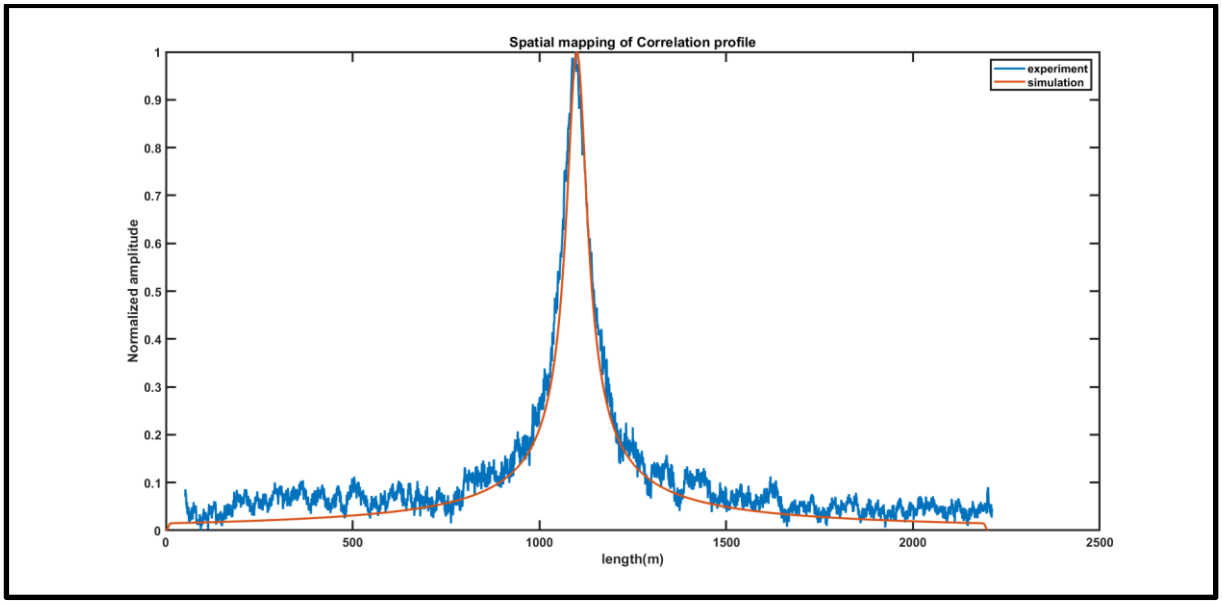

Fig3.04: simulation and experimental verification of zeroth order correlation peak for f_m =10 kHz, Δf =0.532 GHz corresponding to 0.7v pp

Investigating dependence of width of correlation peak on pump pulse width

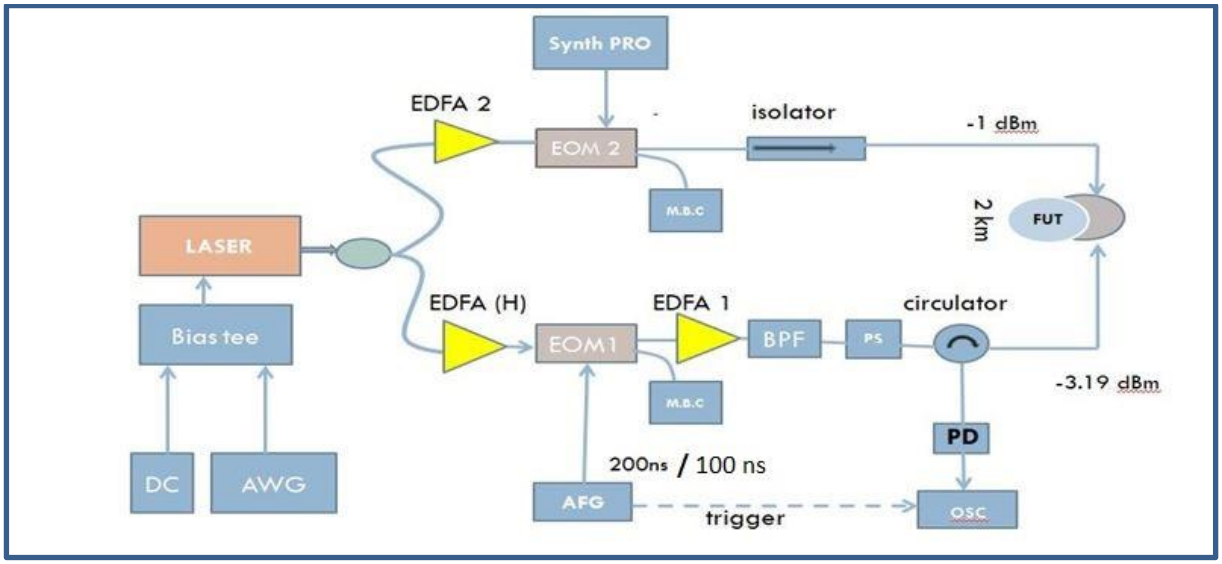

Fig.3.05 Investigating dependence of width of correlation peak on pump pulse width

The Laser used for the experiment is an Eblana Laser at wavelength of 1559 nm, having line width of 2 MHz .The laser is directly modulated by modulating the driving current using an AWG. The bias point is fixed at 4.2V.The light is then split into two arms to generate the pump and the probe light waves. The pump arm is intensity modulated to generate pulses with pulse widths of 200 ns /100 ns at a repetition rate of 25 μs, corresponding to the

round-trip time of the 2km long FUT. The BFS of the 2km fiber is estimated through BOTDA at 10.771 GHz. The probe is frequency shifted with respect to the pump at the BFS itself.

The specifications used for the experimental setup are thus:

f_m= Modulation frequency of pump/probe= **10 kHz**, corresponding to a dynamic range of 10 km.
Length of fiber chosen is= **2.2 km** (exact length estimated through BOTDA measurement)
No. of averages taken= **200**
BFS of the fiber estimated through BOTDA= **10.771 GHz**

Fig.3.06 shows dependence of width of correlation peaks on the pump pulse width used for interrogating the correlation profile. We can observe that the measured width of the correlation profile decreases with decrease in the pump pulse width. This can be attributed to the fact that pulsed pump is used to interrogate the correlation profile & the measured correlation profile is the convolution of the actual correlation profile and the spatial extent of the pump pulse. Thus, smaller the pump pulse width, more accurate is the measured correlation profile.

The FWHM of the correlation peaks are found to be as follows:

For 200ns pulses: 38m, For 100ns pulses: 26m

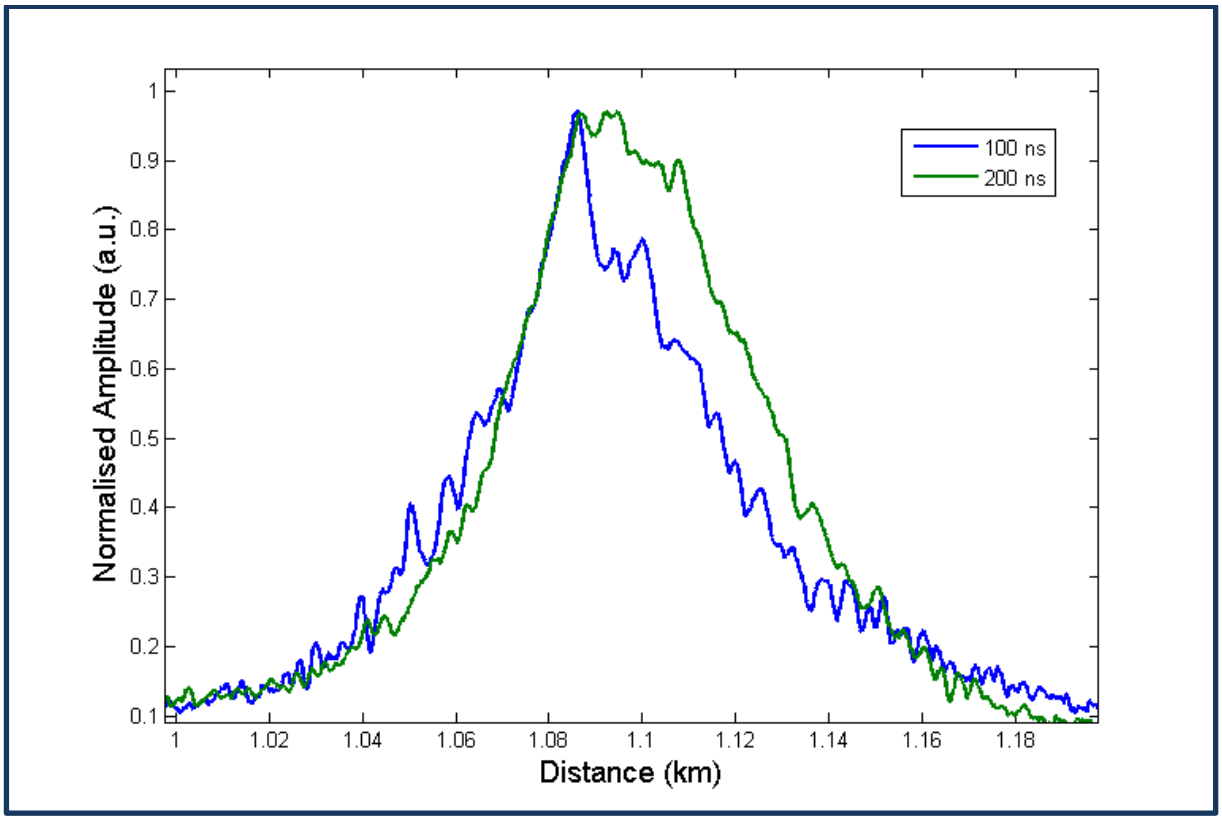

Fig.3.06 Dependence of width of correlation peaks on the pump pulse width

The dependence of the width of correlation peak /spatial resolution on the width of the pump pulse used for interrogating the correlation profile is experimentally verified. As pump pulse width decreases, the width is found to decrease as expected.

The correlation profile can only be mapped with the best spatial resolution of 1m since we are using pulsed pump. This limitation is posed because of the phonon lifetime (10ns). But, when performing actual sensing using BOCDA, we do not use pulsed pump, thus the limitation due to the pulse width of the pump does not pose a constraint in the spatial resolution scenario.

Tunability of correlation peak

Tunability of a single correlation peak in a 2km long fiber is experimentally demonstrated, with change in the modulation frequency for direct modulation of laser. Referring to the same experimental setup, used earlier for spatial mapping and pulse width dependence, tunability of correlation peaks is investigated by tuning the f_m

Modulation frequency of pump/probe is **varied from 24 kHz to 37 kHz**
Length of fiber chosen is= **2.2 km** (exact length estimated through BOTDA measurement).
No. of averages taken= 200 .BFS of the fiber estimated through BOTDA= 10.771 GHz

Length of delay fiber= 6.6 km, Δf= fixed at 1.4 GHz (at 500mV, from previous results)

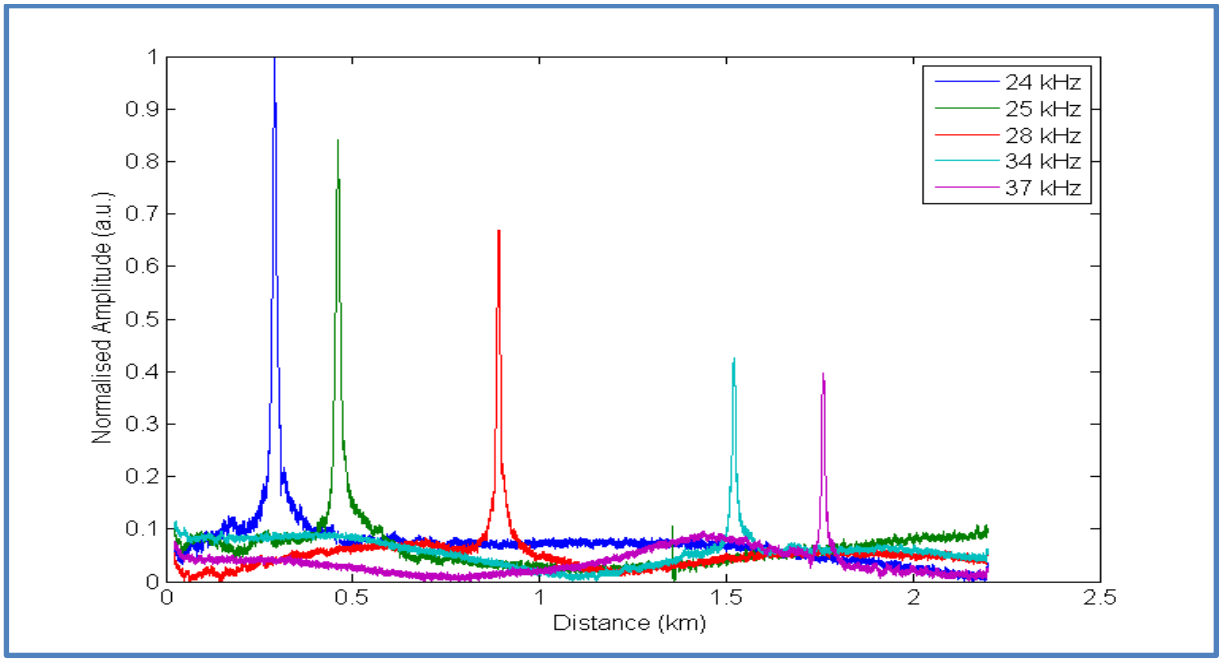

Fig3.07 Tunability of the 1st order correlation peak with change in fm. Pulse width=100ns

From equation below, it is evident that the sensing range can be altered by changing the modulation frequency used for directly modulating the laser source. The dynamic range/sensing range should decrease with increase in the modulation frequency. **Fig.3.07** shows the experimental verification of the same.

$$\Delta z = \frac{c\,\Delta \upsilon B}{2\pi n f m\,\Delta f}$$

$$d = \frac{c}{2nfm}$$

The strength of each correlation peak reduces as we go into the FUT as the pump power decreases along the length of the fiber due to pump attenuation & pump depletion. Also, the peaks become narrower as we increase *f*m , as expected from above equation

Locations of the peaks obtained experimentally: 291m, 461m, 891m, 1.52km, 1.758km

LOCK IN AMPLIFIER (AMETEK 7225)

A lock-in amplifier is a type of amplifier that can extract a signal with a known carrier wave from an extremely noisy environment. Depending on the dynamic reserve of the instrument, signals up to 1 million times smaller than noise components, potentially fairly close by in frequency, can still be reliably detected. Usually sine and cosine demodulation is performed simultaneously, which is sometimes also referred to as dual-phase demodulation (like AMETEK 7225). This allows the extraction of the in-phase and the quadrature component that can then be transferred into polar coordinates, i.e. amplitude and phase, or further processed as real and imaginary part of a complex number. Recovering signals at low signal-to-noise ratios requires a strong, clean reference signal with the same frequency as the received signal

AMETEK 7225 LOCK-IN SPECIFICATIONS:

1. Dynamic reserve: 100 dB

2. Frequency Range: 1 mHz – 120kHz

3. Voltage sensitivity: 2nV – 1V

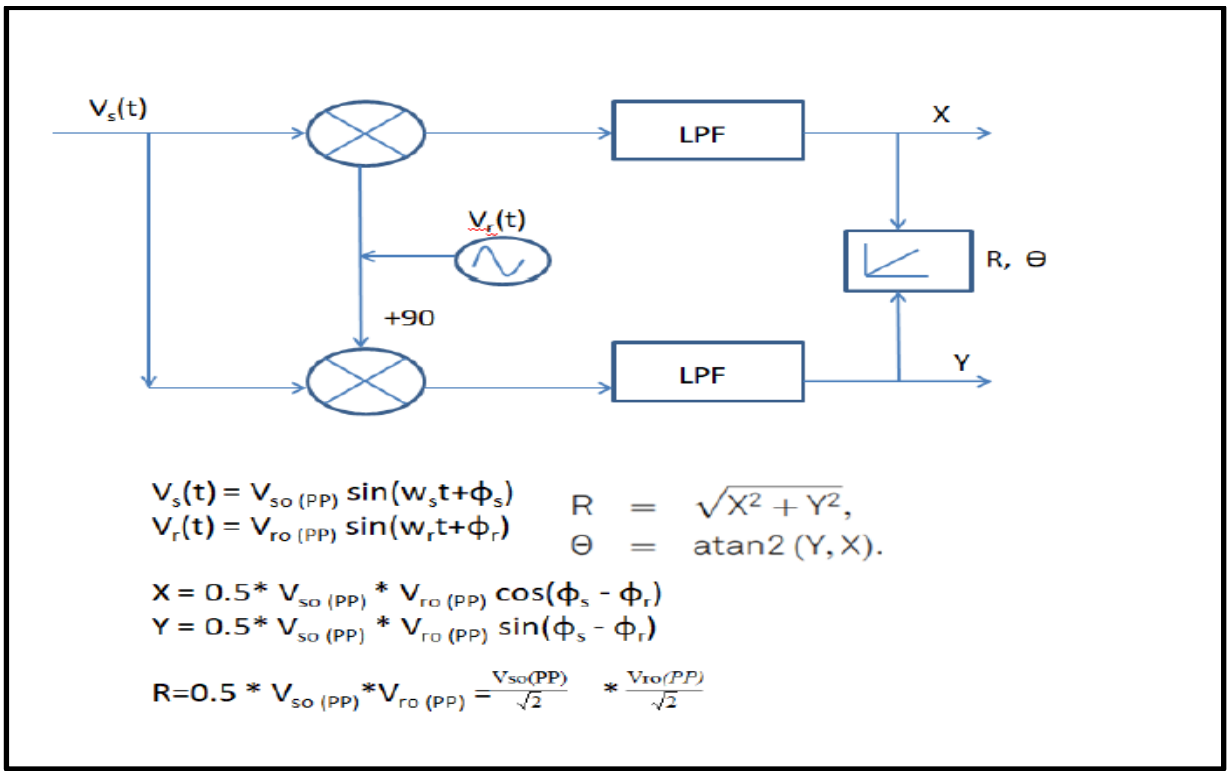

Fig3.08: LOCK-IN amplifier working

The lock-in amplifier multiplies R with $\frac{\sqrt{2}}{Vro(PP)}$ and gives the result as $R= \frac{Vso(PP)}{\sqrt{2}}$

For example, for a sinusoid with PP of 700 mV, an output magnitude of 494 mV is obtained

CHARACTERIZING THE LOCK-IN AMPLIFIER

1. **AM spectral components (carrier and both sidebands)**

fm = 10 KHz

fc = 100 KHz

Carrier amplitude, AC= 460 mV (pp)

Modulation index (m) = 1

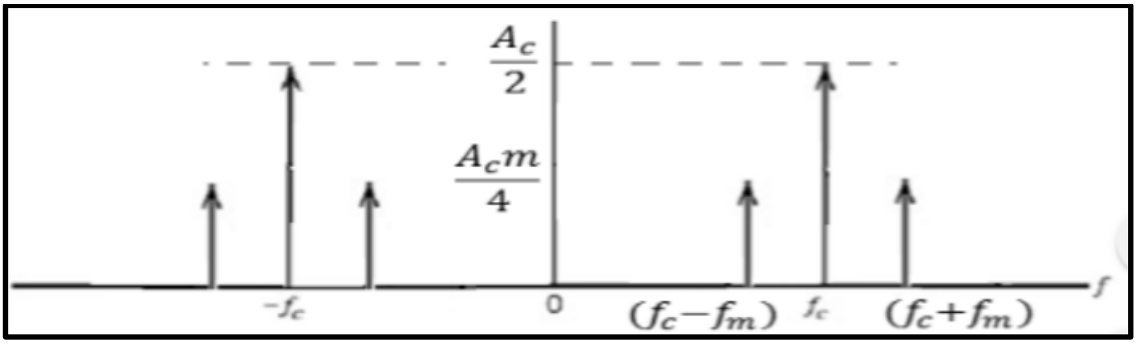

Fig3.09: Typical AM spectrum

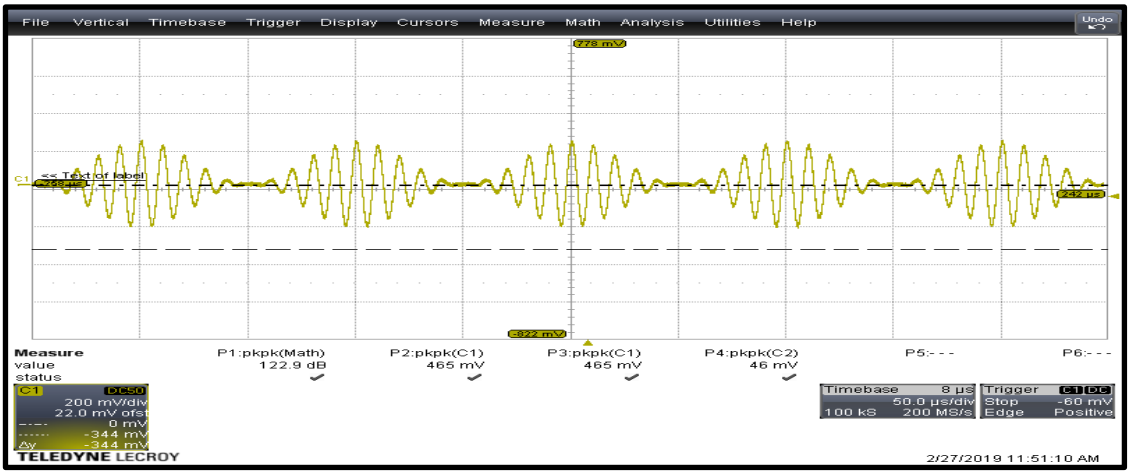

Fig 3.10: Time domain plot of AM signal fed-in

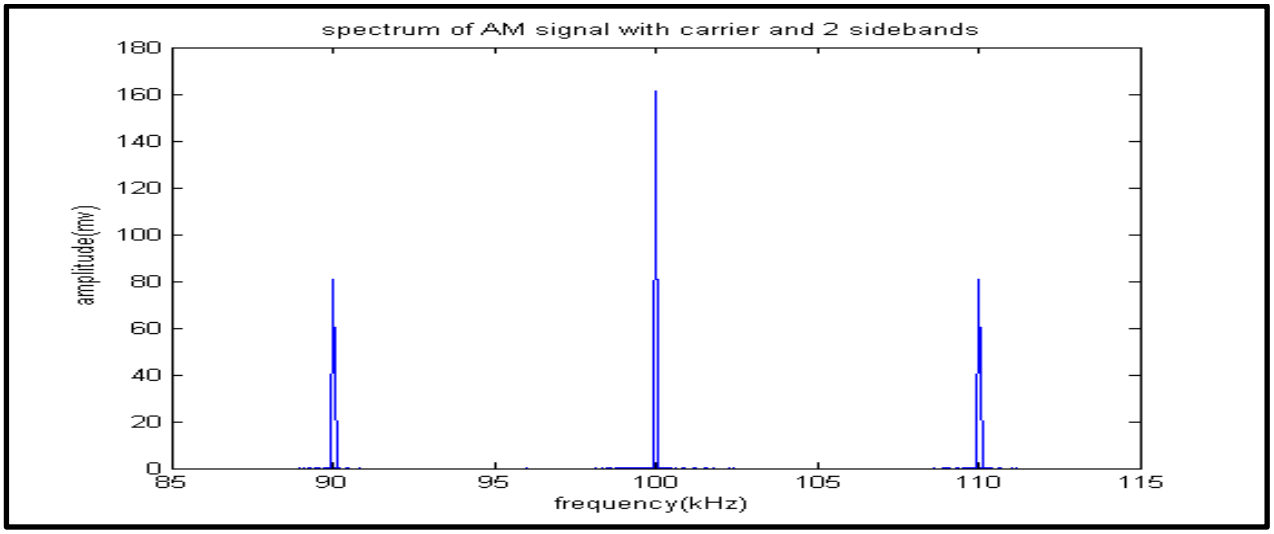

Fig3.11: Received Spectrum of AM signal through Lock-in detection

2. **Sinusoid buried in noise**

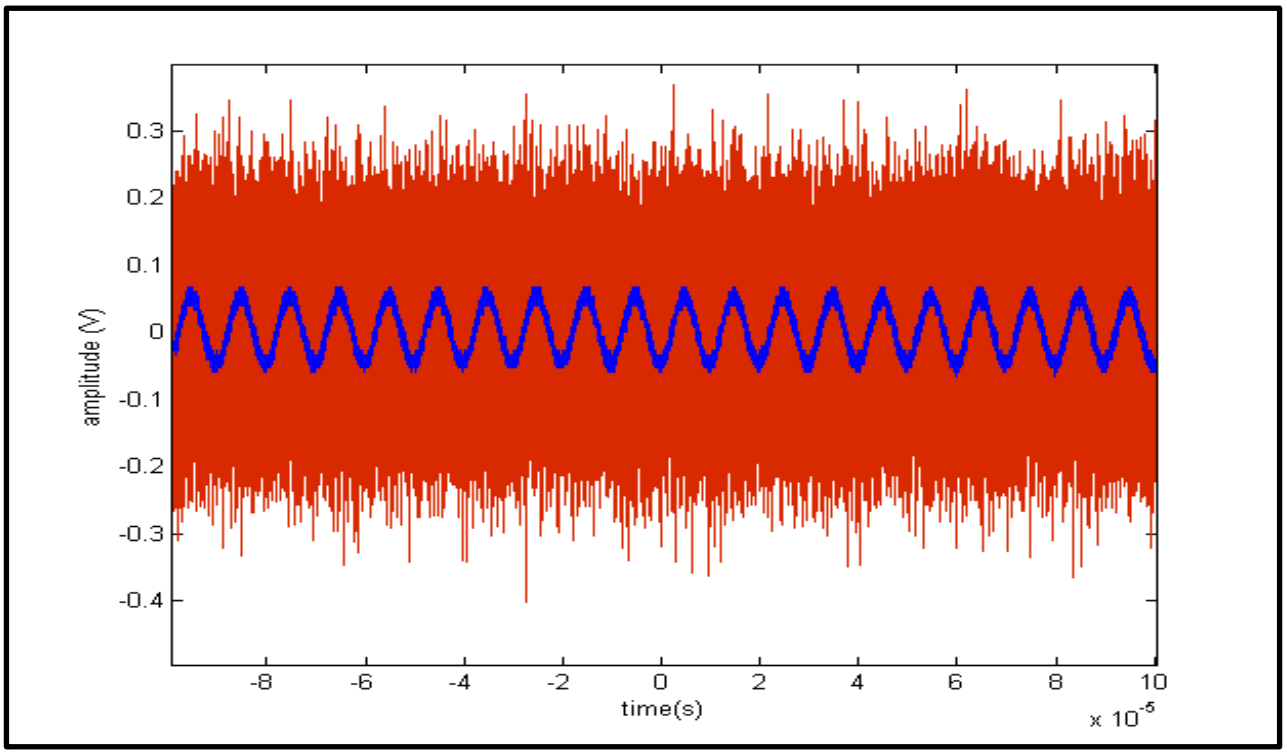

Fig3.12: A sinusoid and a noise signal is fed in to Lock-in amplifier

Noise amplitude: 500mV p-p

Sinusoidal signal amplitude: 100 mV p-p

Extracting the sinusoid buried deep in noise as shown below:

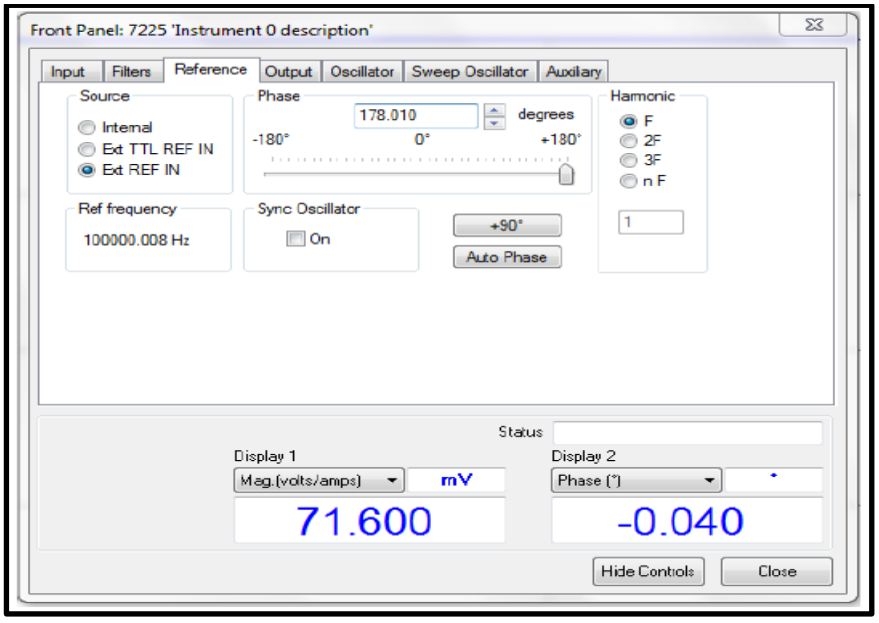

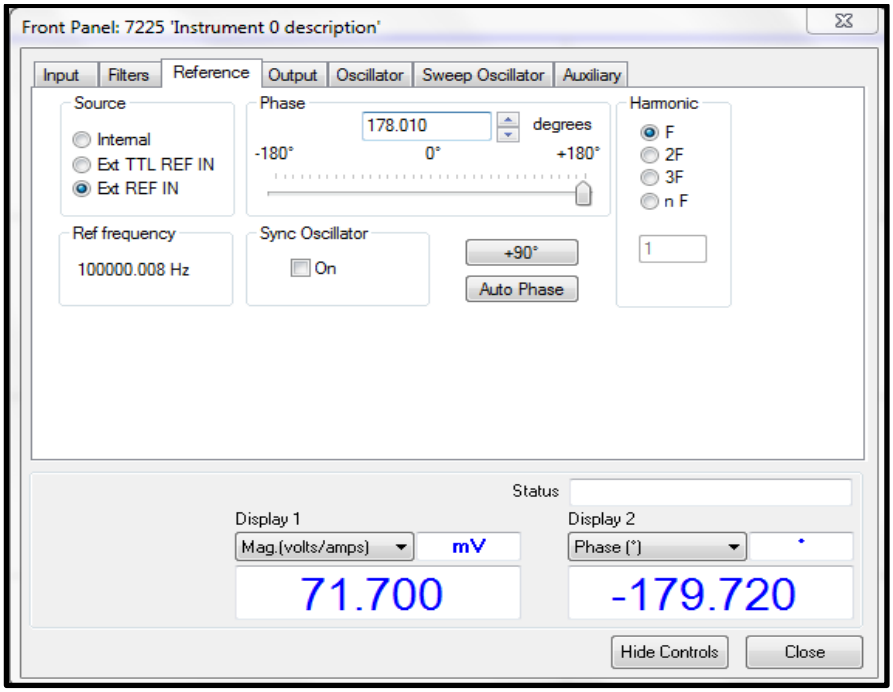

Fig: The phase of the sinusoid detected is also consistent with the phase introduced from the AWG, i.e, when the A,B differential inputs are interchanged the phase gets 180° out of phase

3. Two sinusoids of different frequencies

Two sinusoids of frequency 50 kHz (200 mVpp) and 70 kHz(100 mVpp) were fed in and the spectrum obtained from the lock-in amplifier is shown below:

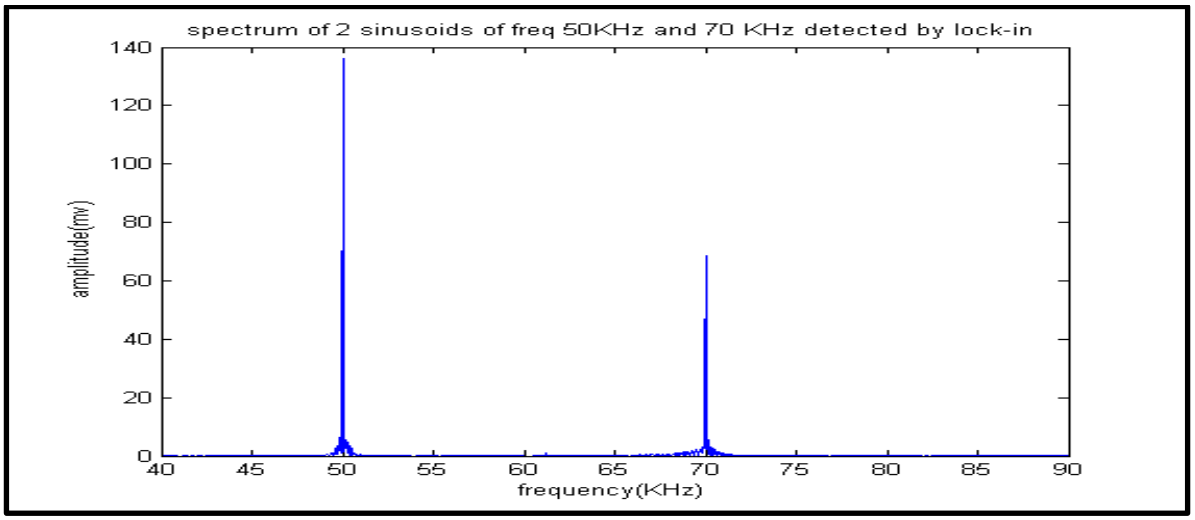

Fig3.13: spectrum of two Sinusoids of different frequencies

Also it was experimentally observed that the lock-in amplifier locks in effectively to a signal only when there is at least a 50 Hz difference between adjacent frequencies. So sinusoids

within 50 Hz frequency difference are indistinguishable, or best achievable frequency resolution is 50 Hz.

4. 1st and 3rd Fourier harmonics of a square wave signal

As we know for a half wave symmetric square wave with no DC offset, spectral peak consists of odd harmonics (1,3,5,…..) and no even harmonics (0,2,4,6…..) and the Fourier amplitude decreases n times 1st harmonic peak ….where n is odd.

Fourier coefficient amplitude = $\frac{2\,V_{PP}}{n\pi}\sin(\frac{n\pi}{2})$

3rd peak will be 1/3rd of the 1st harmonic peak which is verified experimentally as can be observed in the spectrum and also there is no peak corresponding to n=2 (even harmonics)

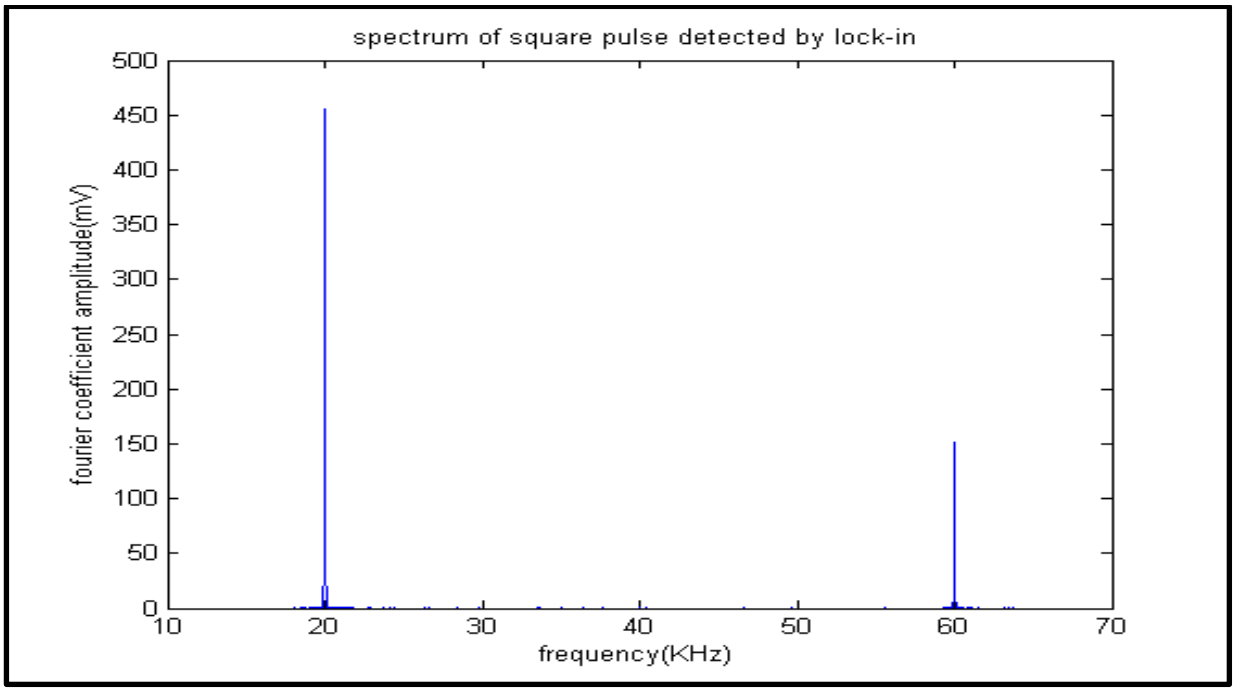

Fig3.14 : Lock-in detection of square pulse

5. External and Internal reference variation with time

It was observed that there were random fluctuations in reference frequency when External reference was generated from the AWG, while the internal oscillator was found to be very stable with no fluctuations at all. Thus, random fluctuations observed earlier in the lock-in output can be attributed to the external reference frequency fluctuations.

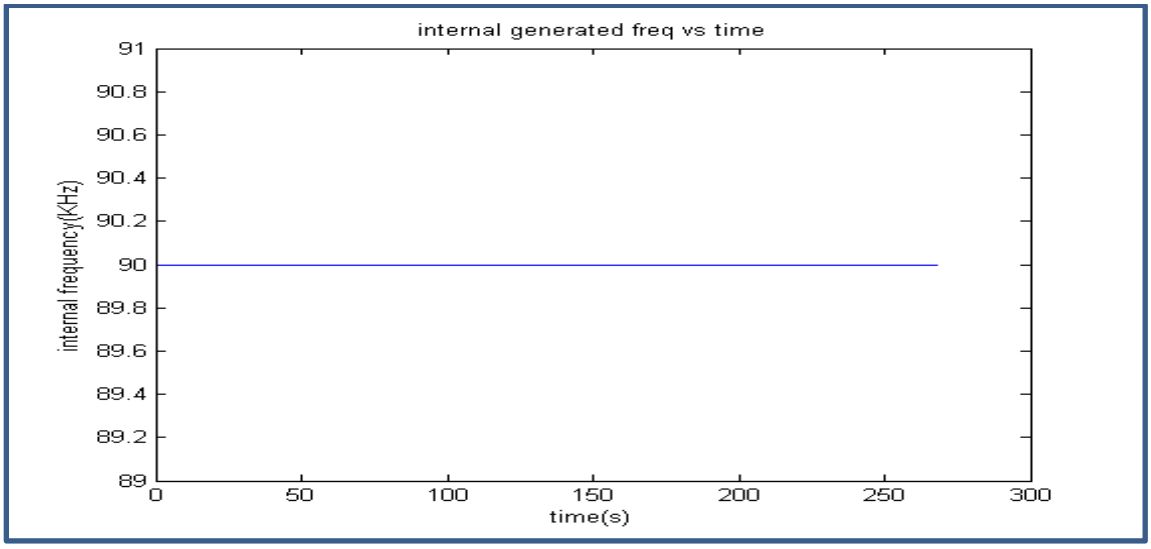

Fig3.15: Internal generated frequency vs time

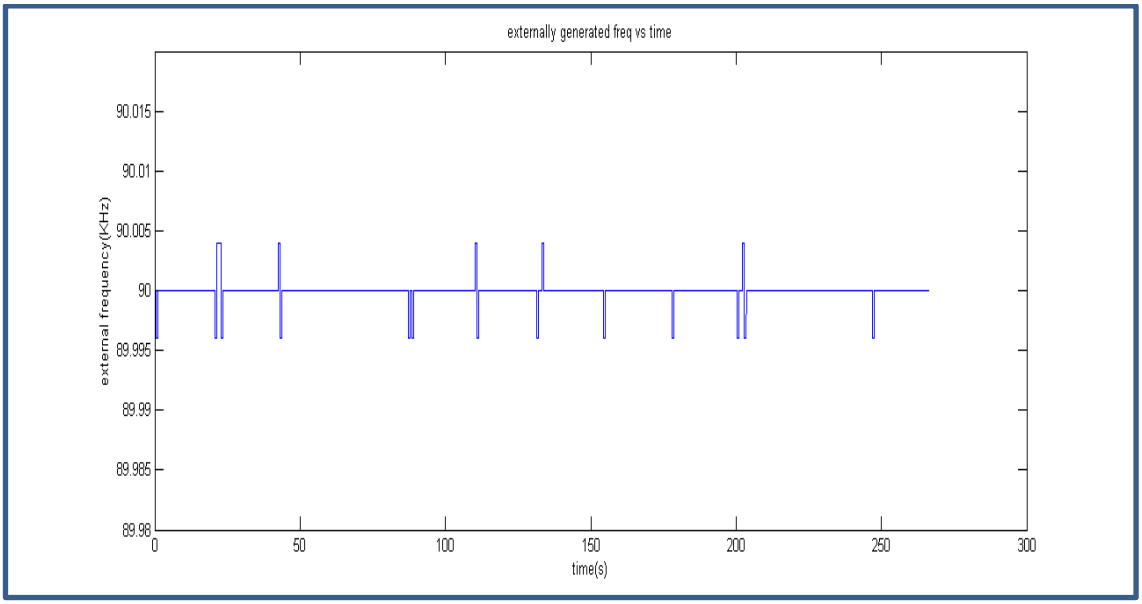

Fig3.16: externally generated frequency vs time

BGS EXTRACTION:

To extract the BGS from the center of a 2km fiber using Direct-modulation BOCDA.

Experimental setup:

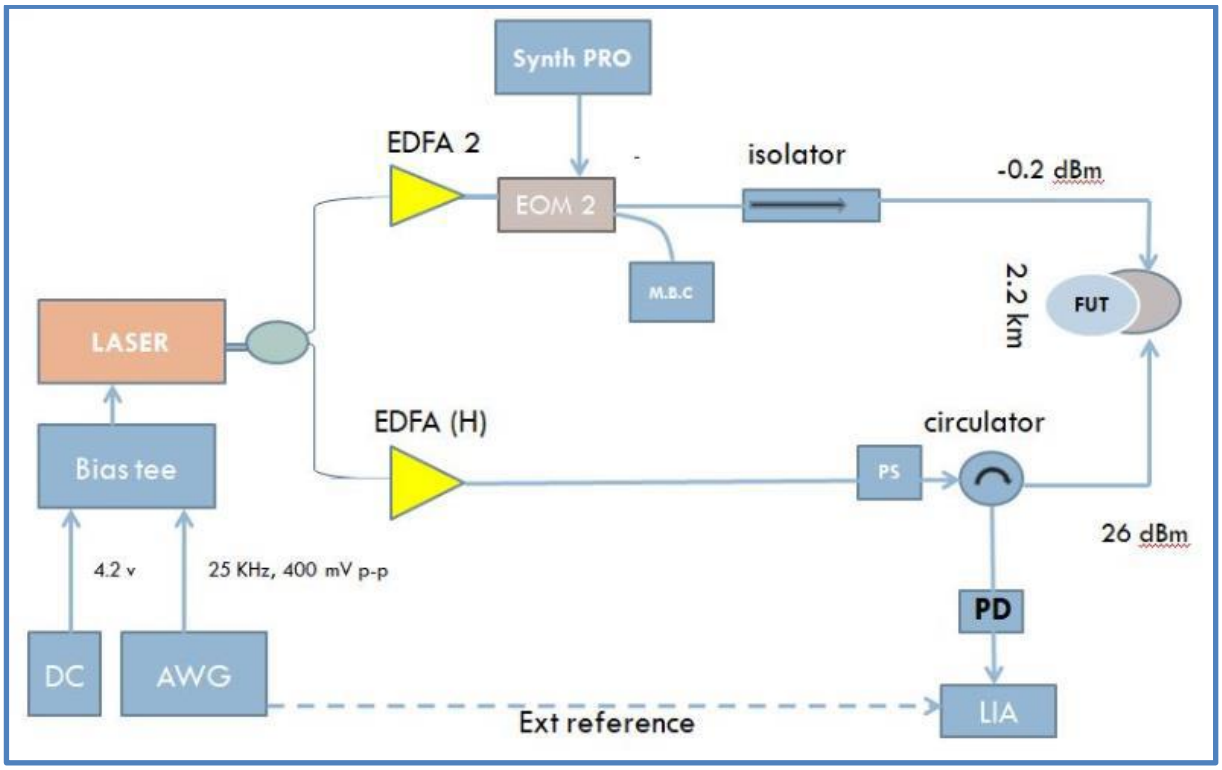

Fig3.17: BGS extraction from 2.2 km fiber through LIA

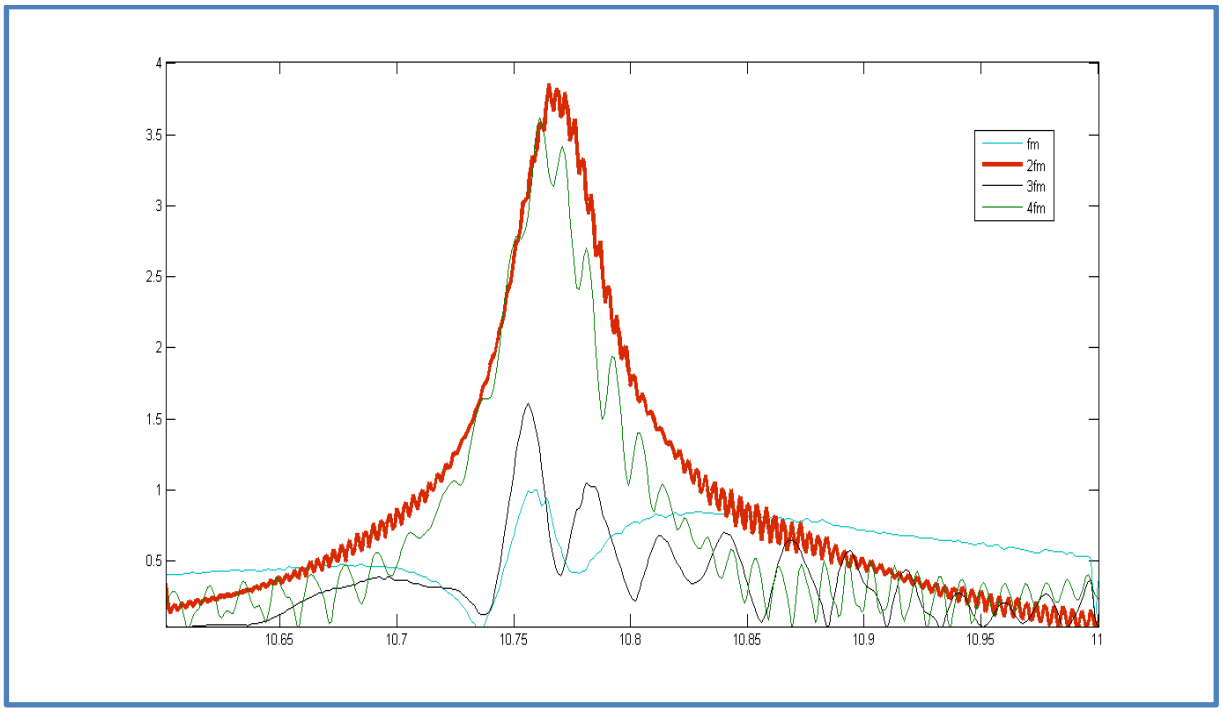

Fig3.18: BGS extracted through Lock-in at different harmonics

Verification with simulations:

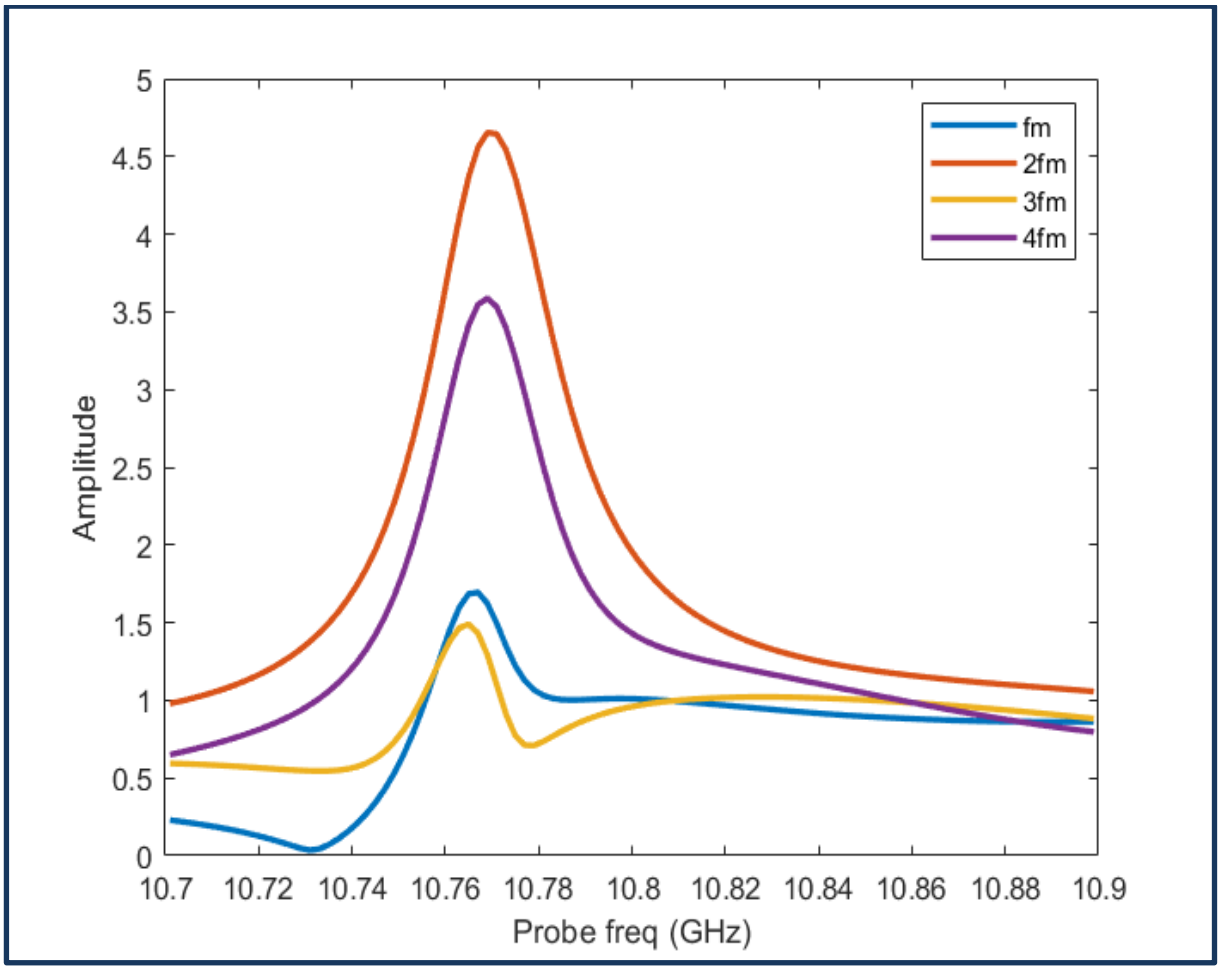

Fig3.19: BGS extracted through Lock-in at different harmonics

The BGS obtained is centred at 10.77 GHz, which is consistent with the results obtained through BOTDA earlier at 10.771 GHz. From the comparison of the extracted BGS for different lock-in frequencies, 2*f*m and 4*f*m frequencies resemble the BGS with a BFS of 10.771 GHz and among the two, the one corresponding to 2fm component exhibits larger strength, leading to potentially higher signal-to-noise ratio (SNR) and hence better accuracy in the estimation of BFS. This is expected because the pump and the probe are frequency modulated at *f*m and are counter propagated in the FUT. The BGS which is formed due to the correlation between the two light waves is expected to have components at 2fm frequency and its harmonics.

Obtaining BGS and checking repeatability in measurement for 2.18 km unstrained section (BFS @2.18 km is around 10.77 GHz)

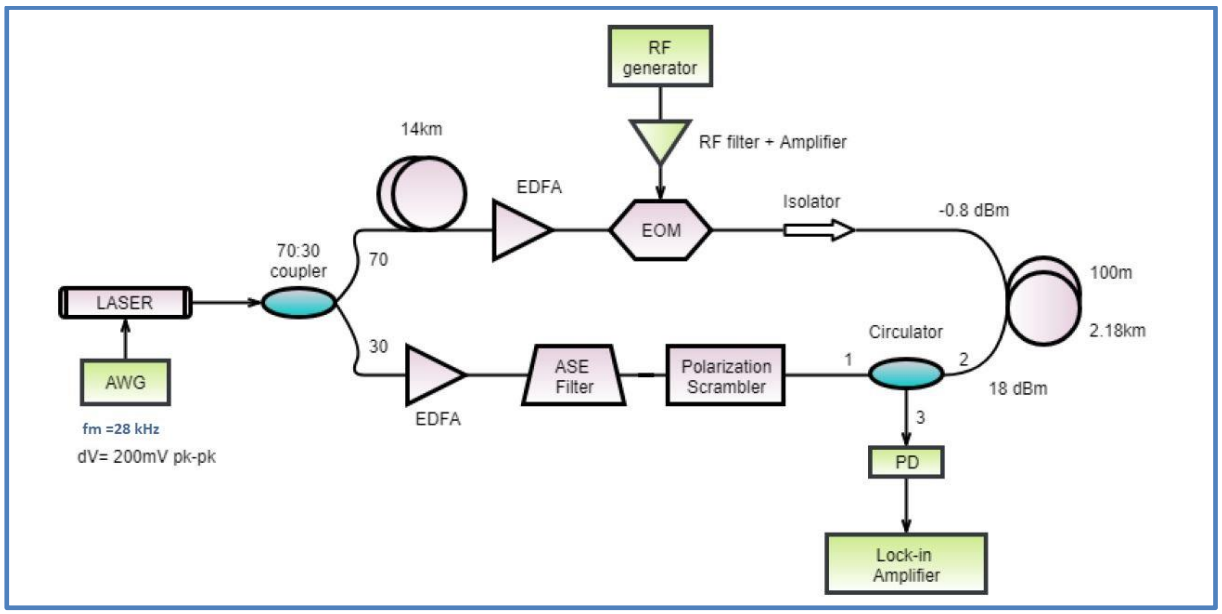

Fig3.20 : Experimental setup of strain sensing

AWG SPECIFICATIONS:

1. *f*m = 28 kHz
2. d= 3.57 km , 2nd order correlation peak formed at 997 m which is well within the 2.18 km fiber
3. Δv pp = 200 mV

LOCK-IN AMPLIFIER SPECIFICATIONS:

1. Time constant = 1s
2. Sensitivity = 10 mV

RF SPECIFICATIONS:

1. Sweep frequency: 10.6 GHz to 10.9 GHz
2. Frequency step = 1MHz
3. Time per frequency step = 1sec
4. Total acquisition time : 300 sec per BGS trace

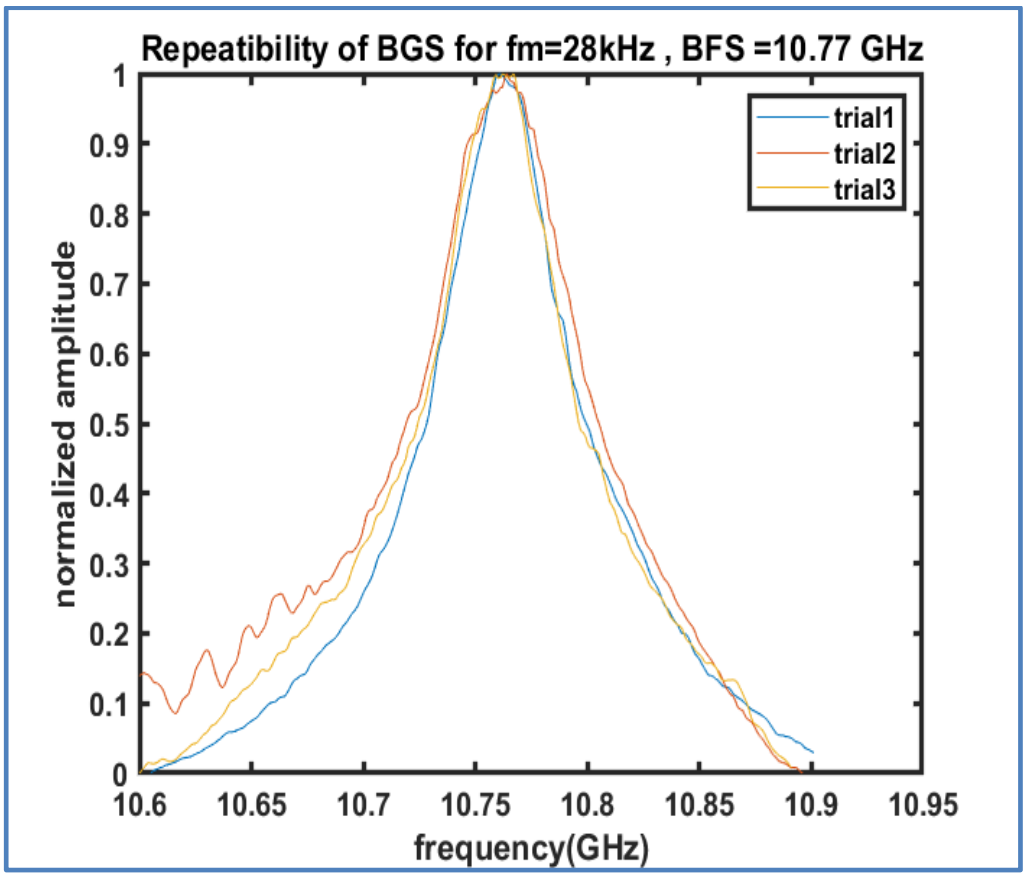

As noted, BFS of 2.18 km section is 10.77±0.015 GHz and is obtained with good repeatability

Obtaining BGS and checking repeatability in measurement for 100m unstrained section (BFS @100m is around 10.73 GHz, verified using BOTDA)

AWG SPECIFICATIONS:

1. *f*m = 28 kHz
2. d= 2.95km , 2nd order correlation peak formed at 2.24 Km which is well within (middle) of the 100m fiber range (2.18Km -2.28 Km)
3. Δv pp = 700 mV

LOCK-IN AMPLIFIER SPECIFICATIONS:

1. Time constant = 1s
2. Sensitivity = 10 mV

RF SPECIFICATIONS

1. Sweep frequency: 10.6 GHz to 10.9 GHz

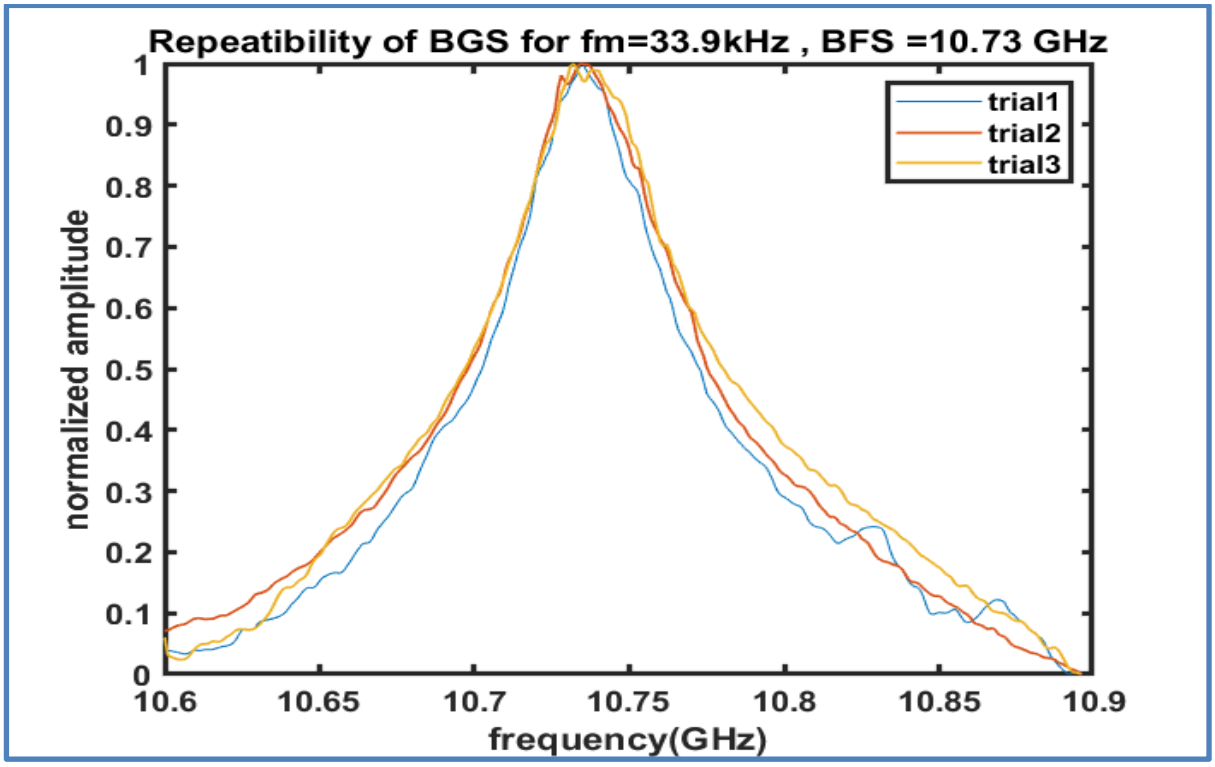

As noted: BFS of 100m section is 10.73±0.002 GHz and is obtained with good repeatability

Applying strain through revolving the ratchet of the screw gauge and obtaining shift in BGS

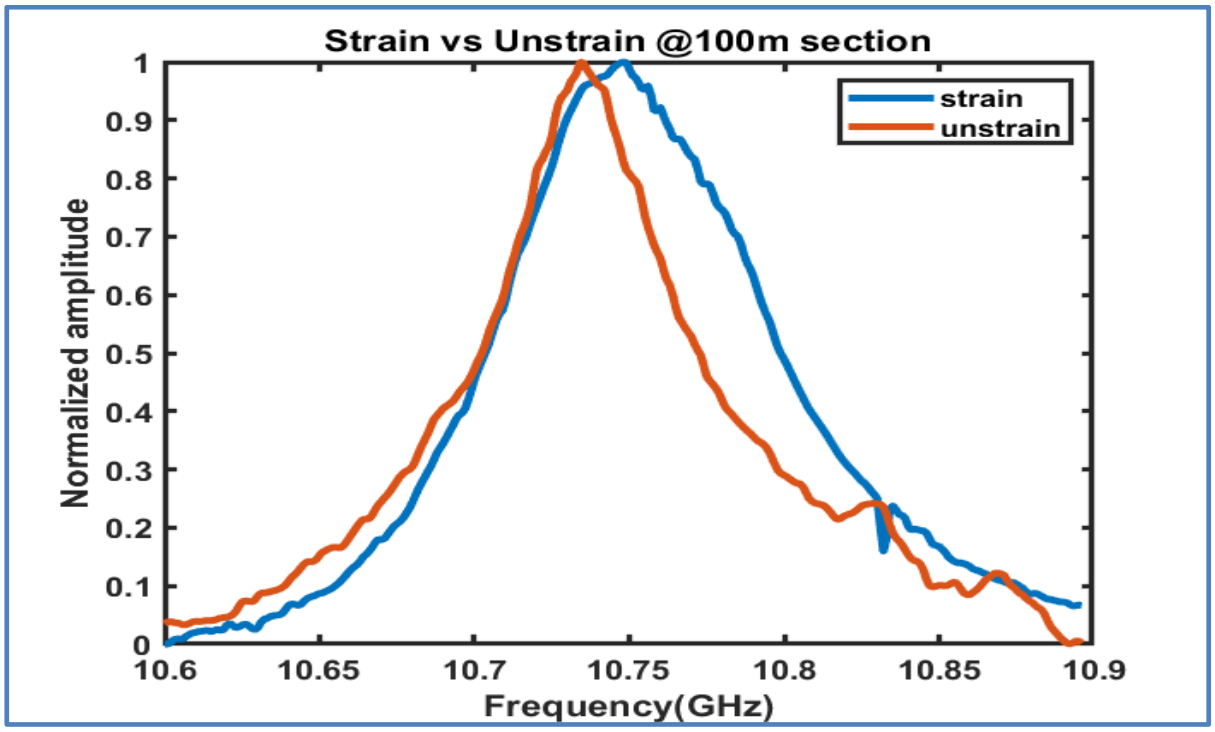

As noted, BFS of 100m section is 10.73 GHz (unstrained) and BFS of strained is around 10.75 GHz. So, shift in BFS of (10.75-10.73) GHz =20 MHz is obtained on applying strain

Repeatability of the BGS at the same micrometer position of the screw gauge (strained position)

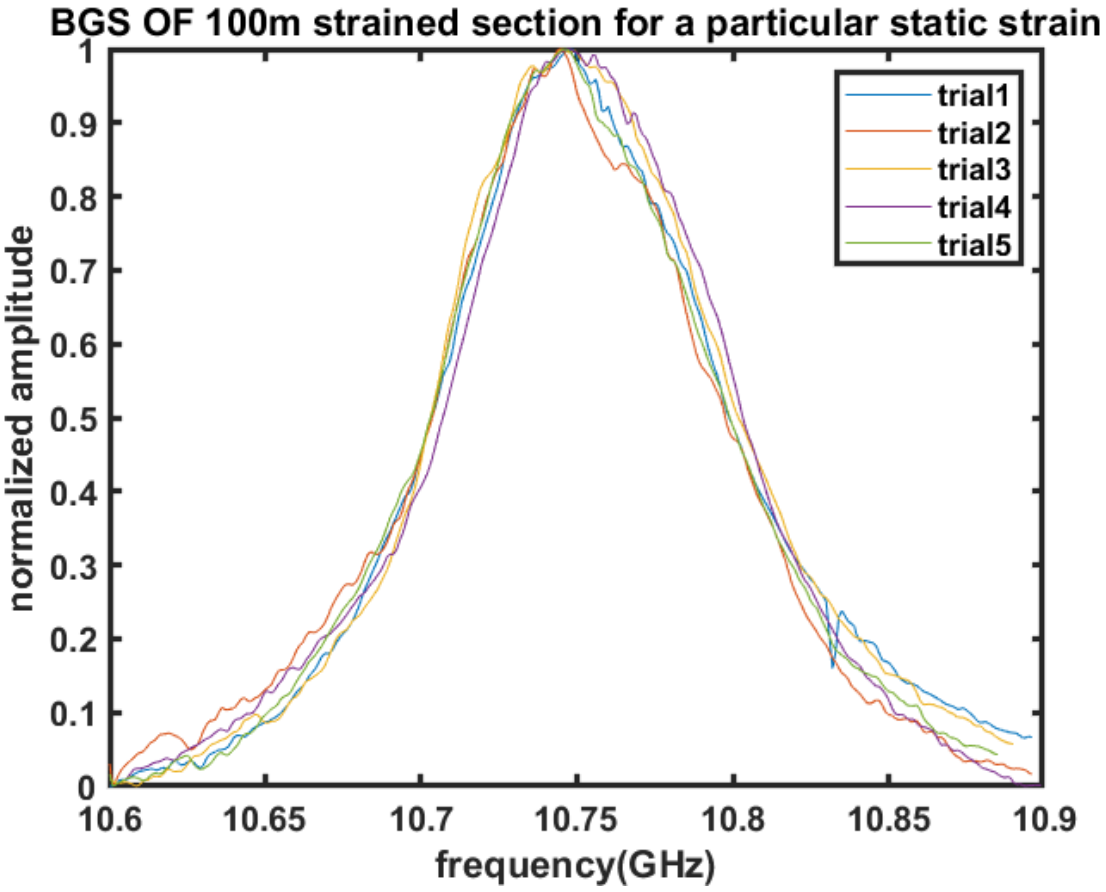

As noted, BFS of strained position is around 10.75±0.0025 GHz which is obtained with good repeatability

Strain coefficient estimation:

1. Strain position 1 : 13.2 mm: BFS :10.73 GHz (considered as unstrained)
2. Strain position 2: 12.8 mm: BFS: 10.735 GHz
3. Strain position 3: 12.4 mm: BFS: 10.74 GHz
4. Strain position 4 : 12.0 mm: BFS:10.75 GHz

l_{sb}= 25 cm = unstrained length of the test bed

ε = δl/l (mS)	δBFS (MHz)
0/25 =0	0
0.4mm/25cm = 1.6	5
0.8/25 = 3.2	10
1.2/25 = 4.8	20

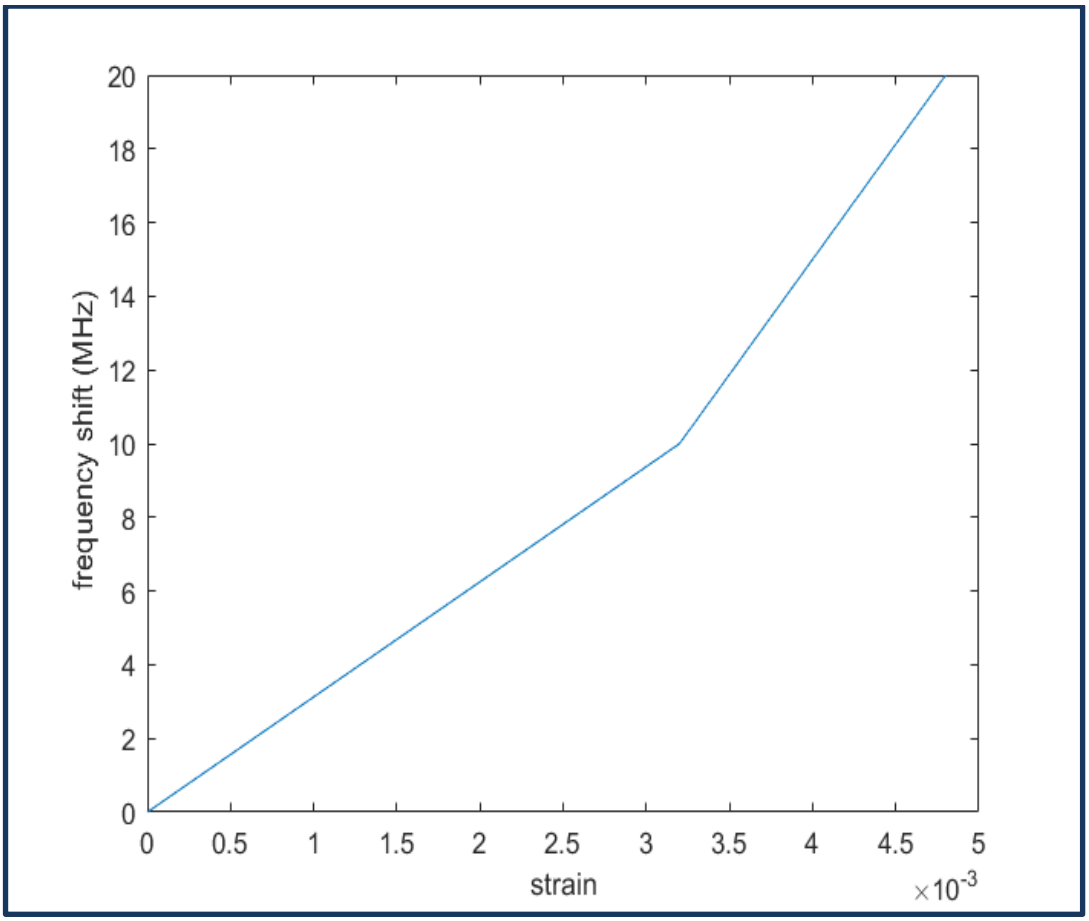

Fig3.21 Plot of frequency shift vs. strain

The strain coefficient is obtained through finding the slope of the frequency shift vs. strain curve which is in order of 50 KHz/ μ strain. Also, the static strain coefficient can be quantified using the recoated FBGs which are interrogated using a broadband light source. Static strain is applied by moving the ratchet of the micrometer screw gauge and observing shift in Bragg wavelength on an OSA (optical spectrum analyser).

SUMMARY & CONCLUSIONS:

In this thesis, Distributed Sensing incorporating Stimulated Brillouin Scattering is exploited. BOTDA technique was used to determine temperature of a hot plate by putting the 12m section of a 10 Km fiber on it. Spatial resolution of 8m was obtained. Since BOTDA suffers from spatial resolution issue as it is a pulsed based , correlation techniques such as BOCDA which has potential of sensing in cm spatial resolution was successfully experimented and also repeatability of measurements were done to check consistency in measurements .

A new Lock-in technique for obtaining Brillouin gain spectrum was investigated. AMETEK 7225 Dual DSP lock-in amplifier was characterized and its functionality was verified with a set of experiments before moving on to capture BGS traces. Two lock-in amplifiers or a Lock-in amplifier & an ESA (zero span mode) is capable of monitoring multiple sensing peaks corresponding to two different modulation frequencies generated by external phase modulation technique .

Simulations on lock-in capture at two different sensing locations are investigated which are ought to be verified using controlled experiments & kept for potential future work .

FUTURE WORK & SCOPE

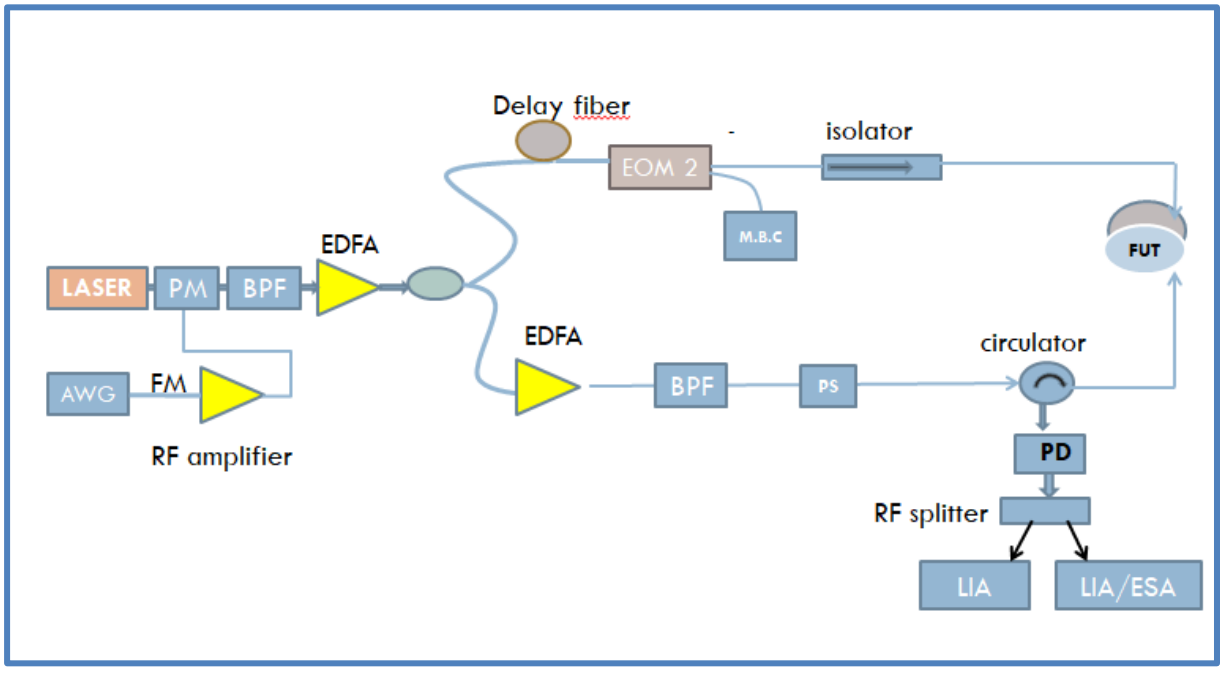

Fig3.22: external phase modulation set up for simultaneous sensing

APPENDIX A

```
clc;
close all;
f_c = 0;
f_m=100e3;           % Modulation freq  in  Hz
delta_f=10e6;        % Freq deviation   in  Hz

sim_time=1e-5;       % Total time of simulation

dt=10e-9;            % Sampling time in sec
c=3e8;               % Velocity of light in vacuum
n=1.5;               % Effective index of fiber
v=c/n;               % Velocity of light in fiber
l=3000;              % Length of FUT in m
dz=dt*v;
delay_fiber=0;    % Length of delay fiber in m

z=dz:dz:l;           % Space discretization
t=dt:dt:sim_time;     % Time discretization

operating_freq=25e6;

for k=1:length(z)
    e_pump(:,k)=exp(1i*((2*pi*(f_c+operating_freq)*(t-
z(k)/v))-((delta_f/f_m)*cos(2*pi*f_m*(t-z(k)/v)))));
    e_probe(:,k)=exp(1i*((2*pi*f_c*(t-(l-
z(k)+delay_fiber)/v))-((delta_f/f_m)*cos(2*pi*f_m*(t-(l-
z(k)+delay_fiber)/v)))));

    beat(:,k)=e_pump(:,k).*conj(e_probe(:,k));
    beat_spec(:,k)=fftshift(fft(beat(:,k)));
end

a=(abs(beat_spec(501:1000,:))).^2/max(max((abs(beat_spec(
501:1000,:))).^2));
plot(z,(a'));

mesh([10.302:0.002:11.3],z,(a'));
xlabel('Frequency (GHz)');
ylabel('Length (m)');
zlabel('Normalized amplitude');xlim([10.3 11.3]);
```

```
for i = 1:length(t)
mu_diff(i,:) =11e9  + delta_f* cos(2*pi*f_m*(t(i)-z/v)) -
delta_f* cos(2*pi*f_m*(t(i)-(l-z)/v));
plot(z,mu_diff(i,:));
hold on;
% pause(0.005);
end

subplot(2,1,1);
plot(z,mu_diff.*10e-10,'linewidth',1);
xlabel('distance');
ylabel('Beat Frequency');
title('Beat frequency and evolution of sensing peaks at
different locations')
subplot(2,1,2);
plot(z,(a'),'linewidth',1);
xlabel('distance');
ylabel('Normalized amplitude');
set(findobj(gcf,'type','axes'),'FontName','Arial','FontSi
ze',12,'FontWeight','Bold', 'LineWidth', 2);
```

APPENDIX B

```
clc
clear
close all
format long
%% Initializing parameters
f_m = 10e3 ; % Modulation freq in Hz
del_f = 0.535e9 ; % Freq deviation in Hz
Dt = 200e-9; % Width of pump pulse in sec
t_r = 25e-6; % Period of pump pulse train in sec
gamma_b = 30e6 ; % Brillouin gain bandwidth in Hz
pump_pow = 0.47e-3 ; % Pump peak power in W
dt = 5e-9; % Sampling time in sec
avg = 200 ; % No. of averages
num = Dt/dt ; % No. of samples in a pulse
c = 3e8 ; % Velocity of light in vacuum in m/s
n = 1.5 ; % Effective index of fiber
v = c/n ; % Velocity of light in fiber in m/ s
l = 2200; % Length of sensing fiber in m
dz = dt*v ; % Step size in space in m
delay_fiber = 6000*0; % Length of delay fiber in m
z = dz:dz:l; % Space discretization in m
t = dt:dt:t_r*avg ; % Time discretization in sec
%% Shaping the pulse with a Gaussian profile
pulse_ampli = [zeros(1,round((t_r/dt-num))/2)
ones(1,round(num)) zeros(1,round((t_r/dt-num))/2)];
%Defining rectangular pulse
gauss_window = gausswin(10) ; % Defining Gaussian profile
gauss_window = gauss_window / sum( gauss_window ) ; %
Normalizing the Gaussian profile
pulse_ampli = conv(pulse_ampli,gauss_window,'same');
%Convolving rectangular pulse with Gaussian profile
pulse_ampli = pulse_ampli/max(pulse_ampli); % Normalizing
resultant pulse
pulse_ampli = [pulse_ampli(round (length (
pulse_ampli)/2)+1: length(pulse_ampli)) pulse_ampli(1 :
round (length(pulse_ampli)/2))]; % Pump pulse shifted to
the start of the array
%% Construction of correlation profile
probe_pow = ones(1,length(z)); % Defining normalized
probe power through out the fiber
```

```
brln_freq = 10.77100e9 ; % BFS of the fiber
operating_freq = 10.77100e9; % Operating frequency

g0=2.5e-11; % Line-center gain coeff
area = 80e-12; %Effective area of fiber
for i = 1 : length(t)
pump_freq = operating_freq+ del_f*sin(2*pi*f_m*(t(i)-
z/v)); % Frequency of pump
probe_freq = del_f*sin(2*pi*f_m*(t(i)-(l-z+
delay_fiber)/v)); % Frequency of probe
freq_shift = pump_freq-probe_freq ; % Beat frequency
between pump and probe
g = g0*( gamma_b/2)^2./ ((brln_freq-freq_shift).^2+(
gamma_b /2)^2) ; % Brillouin gain
probe_pow = probe_pow.*exp(g.* pulse_ampli
(1:length(z))*pump_pow*dz/area) ; % Computation of
amplified probe
back_scattered_pow ( i ) = probe_pow ( 1 ) ; % Extraction
of probe as power of backscattered signal
probe_pow = [ probe_pow(2:end) 1 ] ; % Propagation of
probe
pulse_ampli = [ pulse_ampli(end) pulse_ampli(1:end-1)]; %
Propagation of pump
end
back_scattered_pow = back_scattered_pow-1; % Removing the
initial probe power to get the gain

for i = 1: 2*length(z)
back_scattered(i) = sum(
back_scattered_pow(i:round(t_r/dt):end)); % Averaging the
backscattered signal
end
new_z = linspace(dz/2,l,2*length(z)); % Defining length
axis
back_scattered =  back_scattered-min( back_scattered)
plot( new_z , back_scattered);
xlabel( ' Length (m) ' ) ;
ylabel('Normalized map( a.u.)');
```

APPENDIX C

```
clc ;
clear all;
close all;
% pause on;
 format long;
%% Initializing parameters
f_c1 =6e9 ; % Center freq of FM 1 in Hz
 f_m1=60e3 ; % Modulation freq 1 in Hz
%61khz
del_f1 =0.5e9 ; % Freq deviation 1 in Hz
f_c2 =6e9 ; % Center freq of FM 2 in Hz
f_m2=71e3 ; % Modulation freq 2 in Hz
%70khz
del_f2 =0.5e9 ; % Freq deviation 2 in Hz
t_r=500e-6; % Total simulation time in sec
pump_pow=0.1; % Pump power in W
gamma_b=30e6 ; % Brillouin gain bandwidth in Hz
dt=5e-9; % Sampling time in sec
 c=3e8 ; % Velocity of light in vacuum in m/ s
n=1.5; % Effective index of fiber
v=c/n; % Velocity of light in fiber in m / s
l =1000; % Length of sensing fiber in m
 dz=dt*v; % Step size in space in m
 delay_fiber =13431; % Length of delay fiber in m
z=dz : dz : l ; % Space discretization in m
 t=dt : dt : t_r +2*( l /v) ; % Time discretization in
sec

 %% Modifying the time to account for propagation and
define freq axis

t_new=t(2001:end)-t(2000) ;
fs =1/ dt ; freq=linspace(-fs /2 , fs /2 , length
(t_new)+1) ;
freq_new=freq (1: end-1);

%% Construction of BGS
%
brln_freq=[ones(1,648)*10.8e9,ones(1,20)*10.81e9,ones(1,3
32)*10.8e9]; %for_61khz_strain
%
brln_freq=[ones(1,62)*10.8e9,ones(1,20)*10.81e9,ones(1,91
8)*10.8e9]; %for_70khz_strain
```

```
%
brln_freq=[ones(1,62)*10.8e9,ones(1,20)*10.81e9,ones(1,56
6)*10.8e9,ones(1,20)*10.82e9,ones(1,332)*10.8e9];%simulta
neous_strain
 brln_freq=ones (1 , length (z) )*10.77100e9 ; % BFS of
the fiber
operating_freq =(10.701:0.002:10.900)*1e9 ;  % Operating
freq range
g0=2.5e-11; % Line center gain coeff
area=80e-12; % Effective area of fiber

pump_1=awgn(pump_pow*(1+0.05*sin (2*pi*f_m1*( t ) ) )
,30,'measured') ; % Power of pump 1 with noise
considering residual AM
probe_1=awgn(1*(1+0.05*sin (2*pi*f_m1*(t-delay_fiber /v)
) ) ,30 , 'measured' ) ; % Power of probe 1 with noise
considering residual AM

pump_2=awgn(pump_pow*(1-0.05*sin (2*pi*f_m2*( t ) ) ) ,30
, 'measured') ; % Power of pump 2 with noise considering
residual AM
probe_2=awgn(1*(1-0.05*sin (2*pi*f_m2*(t-delay_fiber /v)
) ) ,30 , 'measured') ; % Power of probe 2 with noise
considering residual AM


 for j =1:length(operating_freq)
                  probe_pow_1=zeros (1 , length (z) ) ; %
Defining normalized probe           power 1 through out
the fiber
                  pump_pow_1=pump_pow*zeros (1 , length
(z) ) ; % Initializing zero pump power 1

                 probe_pow_2=zeros (1 , length (z) ) ; %
Defining normalized probe power 2 through out the fiber
                 pump_pow_2=pump_pow*zeros (1 , length (z)
) ; % Initializing zero pump power 1

                 pump_f1=f_c1+operating_freq ( j
)+del_f1*sin (2*pi*f_m1*t ) ; % Frequency of pump 1
                 probe_f1=f_c1+del_f1*sin (2*pi*f_m1*(t-
delay_fiber /v) ) ; % Frequency of probe 1

                 pump_f2=f_c2+operating_freq ( j
)+del_f2*sin (2*pi*f_m2*t ) ; % Frequency of pump 2
                 probe_f2=f_c2+del_f2*sin (2*pi*f_m2*(t-
delay_fiber /v) ) ; % Frequency of probe 2
```

```
                pump_freq1=(f_c1+operating_freq ( j )
)*ones (1 , length (z) ) ; % Initializing pump freq 1
                probe_freq1=f_c1*ones (1 , length (z) ) ;
% Initializing  probe freq 1

                pump_freq2=(f_c2+operating_freq ( j )
)*ones (1 , length (z) ) ; % Initializing pump freq 2
                probe_freq2=f_c2*ones (1 , length (z) ) ;
% Initializing  probe freq 2

                back_scattered_pow=zeros (1 , length ( t
) ) ;


                for i =1:length(t)
                            freq_shift_11=pump_freq1 -
probe_freq1 ; % Beat frequency between pump 1 and probe 1
                            freq_shift_22=pump_freq2 -
probe_freq2 ; % Beat frequency between pump 2 and probe 2
                            freq_shift_12=pump_freq1 -
probe_freq2 ; % Beat frequency between pump 1 and probe 2
                            freq_shift_21=pump_freq2 -
probe_freq1 ; % Beat frequency between pump 2 and probe 1

                            gain11=g0*(gamma_b/2) ^2./((
brln_freq- freq_shift_11 ) .^2+(gamma_b/2) ^2) ; %
Brillouin gain between pump 1 and probe 1
                            gain22=g0*(gamma_b/2) ^2./((
brln_freq- freq_shift_22 ) .^2+(gamma_b/2) ^2) ; %
Brillouin gain between pump 2 and probe 2
                            gain12=g0*(gamma_b/2) ^2./((
brln_freq- freq_shift_12 ) .^2+(gamma_b/2) ^2) ; %
Brillouin gain between pump 1 and probe 2
                            gain21=g0*(gamma_b/2) ^2./((
brln_freq- freq_shift_21 ) .^2+(gamma_b/2) ^2) ; %
Brillouin gain between pump 2 and probe 1

                            probe_pow_1=probe_pow_1 .*exp
(( gain11+gain21 ) .* pump_pow_1*dz / area ) ; %
Amplification of probe 1 due to SBS

                            probe_pow_2=probe_pow_2 .*exp
(( gain22+gain12 ) .* pump_pow_2*dz / area ) ; %
Amplification of probe 2 due to SBS

                            back_scattered_pow(i
)=probe_pow_1(1)+probe_pow_2(1) ; % Defining
```

```
backscattered power as sum of two probe powers at the
starting of the FUT


probe_pow_1=[probe_pow_1(2:end) probe_1( i ) ]; %
Propagation of probe 1 by a unit length

                                pump_pow_1=[pump_1( i )
pump_pow_1(1:end-1) ]; % Propagation of pump 1 by a unit
length

probe_pow_2=[probe_pow_2(2:end) probe_2( i ) ]; %
Propagation of probe 2 by a unit length
                                pump_pow_2=[pump_2( i )
pump_pow_2(1:end-1) ]; % Propagation of pump 2 by a unit
length

                                probe_freq1 =[
probe_freq1(2:end) probe_f1( i ) ]; % Update frequency of
probe 1
                                pump_freq1=[pump_f1( i )
pump_freq1(1:end-1) ]; % Update frequency of pump 1
                                probe_freq2 =[
probe_freq2(2:end) probe_f2( i ) ]; % Update frequency of
probe 2
                                pump_freq2=[pump_f2( i )
pump_freq2(1:end-1) ]; % Update frequency of pump 2


%
                    end

                               back_scattered_pow_new(:,j)=
back_scattered_pow(2001:end) ; % Discarding backscattered
power until pump & probe enters FUT completely
                               fft_back_scattered_pow(:,j)=
fftshift(fft(back_scattered_pow_new(:,j ) ) )*dt ; % FFT
of backscattered power
 end
     var=operating_freq*1e-9;


plot( operating_freq*1e-
9,(abs(fft_back_scattered_pow(50036,:)*1e3 )
),'linewidth',2 );
 hold on;
```

```
 plot( operating_freq*1e-
9,(abs(fft_back_scattered_pow(50071,:)*1e3 )
),'linewidth',2 );
 hold on;
 plot( operating_freq*1e-
9,(abs(fft_back_scattered_pow(50106,:)*1e3 )
),'linewidth',2 );
 hold on;
 plot( operating_freq*1e-
9,(abs(fft_back_scattered_pow(50141,:)*1e3 )
),'linewidth',2 );
 legend('fm','2fm','3fm','4fm');
                                xlabel ( 'Probe freq
(GHz)') ;
                                ylabel ( 'Amplitude') ;

grid off
set(findobj(gcf,'type','axes'),'FontName','Arial','FontSi
ze',12,'FontWeight','Bold', 'LineWidth', 2);
```